Preliminary Design and Analysis of an Axial Compressor and Matching Turbine Stage for a Gas Turbine

Muhammad Abdullah Zafar Ghauri



NUST
NATIONAL UNIVERSITY
OF SCIENCES & TECHNOLOGY

A report submitted as part of the requirements for the degree
of Mechanical Engineering
at the School of Mechanical and Manufacturing Engineering (SMME)
National University of Sciences and Technology (NUST)
Islamabad, Pakistan

Tuesday 24th June, 2025

Supervisor Dr. Zaib Ali

Abstract

This report focuses on systematic theoretical design of a single-stage axial compressor and the corresponding turbine stage suitable for small gas turbine engine operating under specific specified conditions. The design aims at achieving a compressor ratio of 3.3 while processing air mass flow rate at 0.74 kgs^{-1} with inlet stagnation pressure and temperature of 100 kPa and 300 K, and turbine inlet temperature of 1155 K. The study effectively amalgamates the aerodynamic velocity triangle analysis, thermodynamic energy balances and mechanical work corresponding to ensure that the turbine produces enough power to drive the compressor while compensating for aerodynamic and mechanical losses. Attention is placed on the interconnection between flow angles, blade speed and velocity components in achieving the desired pressure rise and transfer of work. The report also deliberates upon the necessary conditions for maximization of efficiency, potential design trade-offs and mitigation strategies in order to compensate for aerodynamic losses, thereby providing comprehensive and effective engineering solutions. Through analytical derivations, numerical calculations and critical assumptions, this work demonstrates an effective research-based approach to turbomachinery preliminary design.

Acknowledgements

I would like to extend my sincere gratitude to the School of Mechanical and Manufacturing Engineering (SMME) for providing a robust and collaborative academic environment and the resources necessary to undertake this project. I am especially thankful to Dr. Zaib Ali for his invaluable guidance, insightful feedback, and continuous encouragement throughout the course of this design assignment. His mentorship has greatly enhanced my understanding of turbomachinery design principles and their practical applications. This work would not have been possible without his expert supervision and the academic support provided by SMME.

Declaration

I, Muhammad Abdullah Zafar Ghauri, of School of Mechanical and Manufacturing Engineering (SMME), National University of Sciences and Technology, confirm that the work mentioned in this report has been precariously devised with much consultation, deliberation and consensus and the mentioned data including figures, tables, equations, artworks, and illustrations in this report are original and have not been taken from any other person's work, except where the works of others have been explicitly acknowledged, quoted, and referenced. I hereby understand that if failing to do so will be considered a case of plagiarism. Plagiarism is a form of academic misconduct and will be penalized accordingly.

Signed Abdullah Zafar Date Tuesday 24th June, 2025

Muhammad Abdullah Zafar Ghauri

Contents

Abstract ii

Acknowledgements iii

Declaration iv

1 Objectives and Scope 1
- 1.1 Objectives . . . 1
- 1.2 Scope . . . 2

2 Introduction 3
- 2.0.1 Compressors . . . 4
- 2.0.2 Fan . . . 6
- 2.0.3 Pump . . . 6
- 2.0.4 Gas Turbine . . . 6

3 Problem Statement 10

4 Solution Implementation 14
- 4.1 Compressor Stage Preliminary Design . . . 14
  - 4.1.1 Velocity Triangle Analysis . . . 14
  - 4.1.2 Estimation of Pressure Rise . . . 17
  - 4.1.3 Design Discussion 4.1 . . . 22
- 4.2 Turbine Stage Preliminary Design . . . 25
  - 4.2.1 Velocity Triangle Analysis . . . 25
  - 4.2.2 Application of Free Vortex Design to Turbine Stage . . . 27
  - 4.2.3 Reaction of Turbine . . . 31
  - 4.2.4 Evaluation of Temperature Drop and Efficiency Considerations . . . 32
- 4.3 Integrated System Analysis and Trade Offs . . . 33
  - 4.3.1 Matching of Performance by Turbine and Compressor . . . 33

4.3.2 Sensitivity and Trade-Off Analysis 36
4.3.3 Anticipated Losses within Compressor and Turbine Stages 37
4.4 Assumptions Considered for Effective Analysis 41
4.4.1 General Thermodynamic and Fluid Assumptions 41
4.4.2 Compressor Design Assumptions 42
4.4.3 Turbine Design Assumptions 42
4.4.4 Integrated System Assumptions 43
4.5 Integrated System Design 43

5 Conclusion **47**
5.1 Conclusions 47
5.2 Future Work 48

A MATLAB Code Listings for Velocity Triangles and Schematics of Engine Stages **53**

B Project Management **66**

C Project Log **67**

List of Tables

2.1 Identifiers on Centrifugal Pump Schematic 2.3 7

4.1 Variables Involved in analysis of 4.1.1 16
4.2 Variables Involved in analysis of 4.1.2 20
4.3 Variables Involved in analysis of 4.2.1 27
4.4 Variables Involved in analysis of 4.2 31
4.5 Variables Involved in analysis of 4.2.3, 4.2.4 33
4.6 Cumulative Variables Involved in analysis of 4.1 45
4.7 Variables Involved in analysis of 4.2 46

List of Figures

2.1 Examples of turbomachines. (a) Single stage axial flow compressor or pump, (b) mixed flow pump, (c) centrifugal compressor or pump, (d) Francis turbine (mixed flow type), (e) Kaplan turbine, and (f) Pelton wheel. [11] 4
2.2 Dynamic Compressors (Non-Positive Displacement) Compressors [24] . 6
2.3 Sectional view of centrifugal pump schematic [17] 7
2.4 Gas turbine configuration [14] 8
2.5 An open cycle gas turbine engine [15] 9
2.6 A closed cycle gas turbine engine [15] 9

4.1 Velocity Triangles Evaluated at Inlet and Outlet of Compressor 16
4.2 General state of the boundary layer flow over a turbomachine blade [27] 22
4.3 Compressor Blade Cross Section (Side View) 24
4.4 Compressor Blade Cross-Sectional Area 24
4.5 Turbine Velocity Triangles (Inlet and Outlet) 27
4.6 Axial Turbine Blade Cross-Section View 28
4.7 Free vortex rotational flow [25] 28
4.8 Overlaying of Velocity Triangles about the Rotor, Hub and Mean Radius 31
4.9 Schematic of Engine Stage: Compressor and Turbine 44
4.10 Integrated Engine System Schematic 44

Listings

A.1 MATLAB code for evaluation of inlet and outlet velocity triangles of compressor 53
A.2 MATLAB code for devising cross-sectional view of compressor blade . . 55
A.3 MATLAB code for devsiing of compressor blade cross-sectional view . . 55
A.4 MATLAB code for evaluation of inlet and outlet velocity triangles of turbine 56
A.5 MATLAB code for overlaying of velocity triangles about hub,rotor and mean radius 58
A.6 MATLAB code for devsiing turbine blade cross-section 60
A.7 MATLAB code for engine stage comprsing of compressor and turbine . 61
A.8 MATLAB code for integrated engine system schematic with necessary annotations 63

Chapter 1

Objectives and Scope

A short paragraph introducing the topic the chapter examines.

1.1 Objectives

The main objective of this assignment is to deliberate and design a single-stage axial compressor and corresponding gas turbine stage suitable for meeting the performance requirements of a small gas turbine engine operating under certain specific operation conditions. Specifically, the objectives are:

- To determine the velocity components and evaluate inlet and outlet velocity triangles corresponding to turbine and compressor stages
- To calculate the pressure rise within compressor and enthalpy drop in turbine by incorporating real-world factors affecting the efficiency.
- To ensure the work matching between turbine and compressor while accounting for mechanical coupling efficiency and aerodynamical losses.
- To analyze the influence of blade angles, velocity components and reaction degree on the performance and efficiency of both stages critically.
- To identify the factors corresponding to aerodynamical and mechanical losses and suggest adequate strategies for minimization of such losses.
- To suggest a technically sound and realistic design supported by detailed derivations, diagrams and professional discussion.

1.2 Scope

The scope of this report comprises of preliminary design of single-stage axial compressor and corresponding turbine stage suitable for gas turbine operating at a compressor ratio of 3.3 while processing air mass flow rate at 0.74 kgs^{-1} with inlet stagnation pressure and temperature of 100 kPa and 300 K, and turbine inlet temperature of 1155 K. The design approach tends to incorporate the considerations for devising velocity triangles, the application of Euler's turbomachinery equation, energy balance analysis and efficiency correlations. The study effectively considers important aerodynamical assumptions such as constant axial velocity and ideal velocity triangle relations while integrating practical efficiency factors in order to reflect real-world performance. The analysis also aims at exploring the sensitivity of design parameters and discussing important trade-offs in adequate selection of flow angles, reaction degree and blade speed. Since this report suggests for design considerations, therefore software analysis, such as Computational Fluid Dynamics (CFD), structural and thermal analysis while it focuses on aerodynamical and thermodynamical design considerations in order to achieve a well-balanced, efficient and technically justified turbomachinery design.

Chapter 2

Introduction

Turbomachinery, serves an important in mechanical engineering and a practical aspect of fluid mechanics [9], describes the machines which effectively transfer energy between fluid and dynamic rotor, which comprises of both compressors and turbines. Turbines are used for transferring energy from fluid to rotor while compressors are used for transferring of energy from rotor to fluid [21][30]. The entire concept of turbomachinery revolves around Newton's second Law of Motion and Euler's turbomachinery equation for compressible fluids. In addition to compressors and turbines, centrifugal pumps are also considered an important part of turbomachinery which transfer energy from rotor to fluid(primarily in liquid form), while compressors and turbines usually work with gas. In general, the turbomachines are categorized in terms of configuration, open and closed, where in case of open machines such as propellers, windmills and fans act on infinite extent of fluid flow, whereas in case of closed machines, they operate on finite quantity of fluid as it passes through the casing or housing. In addition to construction configuration, the classification can be done on the basis of type of flow. When the flow is parallel to axis of rotation, they are called axial flow machines, while when the flow is perpendicular to axis of rotation, they are called radial flow machines. For machines involving both the axial and radial flow of fluid, they are referred to as mixed flow machines [30]. in addition, the turbomachines can be further classified into two additional categories, ones whcih absorb energy in order to increase fluid pressure, referred to as pumps, fans and compressors and others which produce energy such as turbines by expansion of flow to low pressures [5].

Turbomachines serve as an important part of every energy system by effectively transferring energy between a rotor and a fluid (gas or liquid). The enrgy transfer can take place from rotor to fluid (in compressors, fan or pump) or from fluid to rotor (in gas and steam turbines). In order to minimize leakage losses, modern turbomachines have

smaller gaps between rotor and casing. In case of pump, the pressure of incompressible fluid is increased to a hugh level, while the pressure of compressible fluid is increased by means of a compressor. According to ASME standards, fans tends to differ from blowers and compressors by the pressure ratio, which can be 1.1 for fans, 1.11-1.2 for blowers and more than 1.2 for compressors. In case of steam turbine, the superheated steam undergoes expansion, leading ro mechanical work being done. There is a combustion chamber embedded in gas turbine, which coverts the fuel to mechanical energy by spontaneous and non-spontaneous combustion reactions [3].

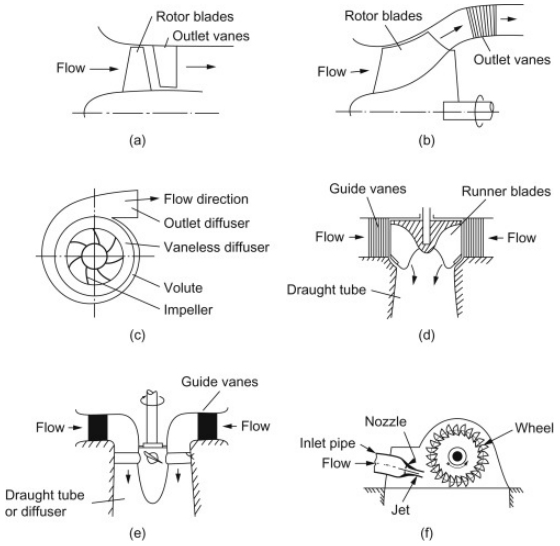


Figure 2.1: Examples of turbomachines. (a) Single stage axial flow compressor or pump, (b) mixed flow pump, (c) centrifugal compressor or pump, (d) Francis turbine (mixed flow type), (e) Kaplan turbine, and (f) Pelton wheel. [11]

2.0.1 Compressors

Compressors are extensively used in order to increase the pressure and enthalpy of compressible, low density fluids with the pressure increase being characterized by compressor pressure ratios which describe the ratio of outlet pressure, referred to as discharge pressure to the inlet pressure, referred to as suction pressure. They are classified into two major categories, respectively as positive displacement (for intermittent flow) and dynamic machines (for continuous flow). Positive displacement compressors consist of rotary and reciprocating compressors, while dynamic compressors consist of centrifugal and axial compressors. The rotary compressors consist of two rotors embedded within casing, while the reciprocating compressors increase pressure of moving fluid by reducing the volume, by means of piston encased in a cylinder as a compressing and displacing element, thereby achieving high compression ratios. Centrifugal compressors tend to convert the transmitted angular momentum by set of rotating impeller blades

to the working fluid. They use set of aerofoils to effectively compress the working fluid. Basically, the compressor model has one inlet flow and one outlet flow, hence the mass flow rate through the inlet and the outlet remians constant:

$$\dot{m}_{in} = \dot{m}_{out} \tag{2.1}$$

The energy balance equation can be expressed as:

$$\dot{m}_{in} h_{in} = \dot{m}_{out} h_{out} + P \tag{2.2}$$

Where P is the performance parameter and it can be calculated as:

$$P = \dot{m} c_p(\bar{T}) T_{in} \Omega_{comp} \tag{2.3}$$

where $\bar{T}$ is the average temperature, evaluated at the inlet of compressor and outlet of compressor.

$$\bar{T} = \frac{T_{in} + T_{out}}{2} \tag{2.4}$$

The dimensionless parameter Ω_{comp} can be expressed as:

$$\Omega_{comp} = \Pi^{\frac{\kappa}{\eta_{poly,comp}}} \tag{2.5}$$

Where κ is referred to as isentropic constant, and Π being the optimum pressure ratio dependent upon the thermodynamical model serving as the basis of further analysis and should provide the maximum efficiency of gas/steam processes.

$$\eta_{poly,comp} = \kappa \frac{ln(\Pi)}{ln(\frac{\Pi^{\kappa}-1}{\eta_{isen,comp}} + 1)} \tag{2.6}$$

where $\eta_{isen,comp}$ is the isentropic efficiency of compressor:

$$\eta_{isen,comp} = \frac{h_{out} - h_{in}}{h_{out,isen} - h_{in}} \tag{2.7}$$

The discharge temperature of compressor can be evaluated using following formula:

$$T_{out} = (1 + \Omega_{comp}) T_{in} \tag{2.8}$$

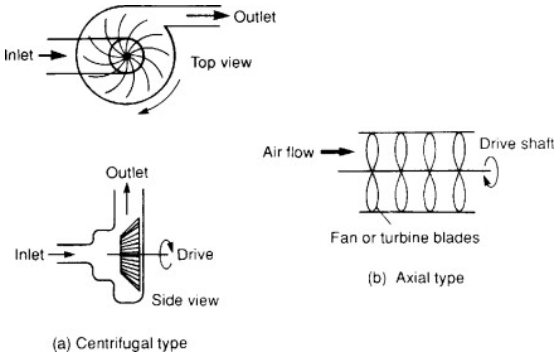


Figure 2.2: Dynamic Compressors (Non-Positive Displacement) Compressors [24]

2.0.2 Fan

Fans are generally used to generate pressure difference, allowing for large mass flow rates of fluid to overcome the flow resistance in an effective manner. The driving power for fan is supplied by rotating shaft (which is usually accomplished by an electric motor). Fans are further classified as axial and radial fans, in case of axial fans, the flow of fluid is in axial direction along the fan shaft without cha ge in flow direction, while in case of centrifugal fan , the fluid flow tends to change its direction relative to the shaft [3].

2.0.3 Pump

Pumps are specifically designed un order to increase the pressure of flowing incompressible fluids, with high density such as water and oil, while compressors are most suitable for compressible, low-density fluids such as air or gas. The mechanical energy of shaft is transformed into kinetic and potential energy of flow by a pump. Within a thermal energy plant, pumps are used for transmission of working fluid from one location to another. For example, condensate pumps transmit condensate water through low-pressure preheaters into feedwater storage tank. The boiler feedwater pump forces water from feedback water rank to flow through high-pressure preheaters prior to entrance into steam generator. In order to ensure effective operation of centrifugal pumps, there is an immense requirement of high-grade load to ensure highly efficient performance with one decreasing as the load decreases.

2.0.4 Gas Turbine

Gas turbine is an essential and one of most important applications of turbomachinery, which is generally used for power-production. It utilizes energy contained in fuel such as oil or gas, either the kinetic energy due to motion of fluid or the potential energy of fluid subjected to pressure in order to generate necessary rotary motion [8]. Generally, a gas turbine consists of three major components:

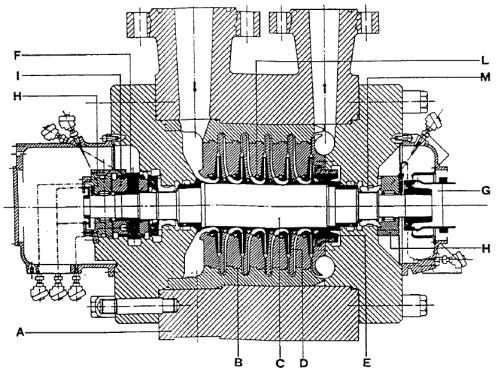


Figure 2.3: Sectional view of centrifugal pump schematic [17]

Table 2.1: Identifiers on Centrifugal Pump Schematic 2.3

Nomenclature	Identifiers
A	Outer Casing
B	Diaphragm Bundle
C	Shaft
D	Impellers
E	Balance Drum
F	Thrust Collar
G	Hub
H	Journal Bearing
I	Thrust Bearing
L	labyrinth Seals
M	Oil Film End Seals

- Rotating gas compressor
- Combustor
- Compressor-driving Turbine

In addition to the above mentioned compulsory components, certain gas turbines designed for specific applications have additional components. In order to provide additional thrust to an aircraft in flight, a propelling nozzle is used along wit an additional turbine to drive the propeller or ducted fan in order to conserve fuel consumption by increasing the propulsive efficiency at subsonic flight speeds. Considering a helicopter, an additional turbine is used to drive the helicopter rotor or land-vehicle transmission (turboshaft), marine propeller or electrical generator. By addition of afterburner, one may achieve high thrust-to-weight ratios. The fundamental working principle behind a gas turbine is the Brayton's cycle with air acting as the main working fluid. Air flows through the compressor which compresses it to high pressure followed by addition of

extra energy by combustion of fuel in presence of air, the combustion generates high-temperature flow which enters the turbine, producing the shaft work output in process, thus driving the compressor and the unused energy is moved outwards the system by means of exhaust which can be used later or dumped into atmosphere. The purpose of the gas turbine determines the design so that the most desirable split of energy between the thrust and the shaft work is achieved [32][28]. The following figure 2.4 shows a gas turbine with regenerator which uses generator exhaust vapors to preheat air exiting the compressor, thereby reducing the amount of fuel required by gas turbine. The same figure shows the changes associated with gas temperature, pressure, energy, and the horsepower produced in the different sections of the gas turbine. The power produced in gas turbine is typically three times the output power as the air compressor generally requires two-thirds of generated power. Gas turbines are generally classified as open

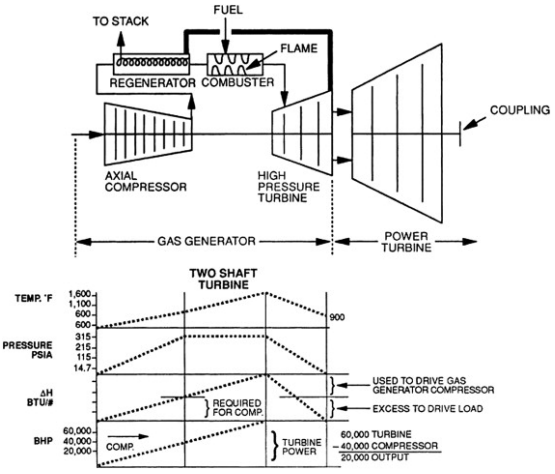


Figure 2.4: Gas turbine configuration [14]

cycle and closed cycle gas turbines

Open Cycle Gas Turbine

In open cycle gas turbines, fresh atmospheric air is drawn into the compressor at ambient conditions followed by compression using an axial or centrifugal compressor. The compressor increases the temperature and pressure of atmospheric air which is later fed to a combustion chamber where the combustion of fuel takes place at constant pressure. The high-pressure gas drives the turbine and generates power due to rotation of turbine which can be later utilized for various applications such as power generation. The exhaust gases leaving the system are released into atmosphere, thereby classified as open-cycle system as the exhaust gases are nor recirculated but released into the atmosphere [2], [1].

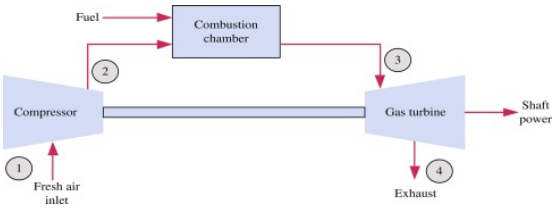


Figure 2.5: An open cycle gas turbine engine [15]

Closed Cycle Gas Turbines

In closed cycle gas turbines, by means of compressor, the pressure and temperature of inlet air is increased. The high-pressure compressed air enters the heat exchanger, where heating is done by means of an external source. The high pressure and temperature air are fed into the turbine, where expansion takes place. The power generated within a closed-system due to high-pressure fluid increases across the turbine. The exhaust working fluid is not released into the atmosphere, rather it is cooled using a cooling chamber and recirculated for continuous operation within the system. The cycle is termed close-gas turbine system as the same working fluid is returned back into compressor prior to completion of process.

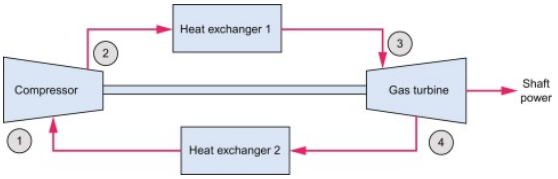


Figure 2.6: A closed cycle gas turbine engine [15]

Chapter 3

Problem Statement

Design Requirements

Design a single-stage axial compressor and a corresponding turbine stage that drives the compressor. The design should meet specified performance targets and demonstrate the interplay between aerodynamic design, energy transfer, and efficiency. The assignment requires both conceptual justification and numerical analysis.

A small gas turbine engine is required to operate at the following conditions:

- **Mass Flow Rate:** $\dot{m} = 0.74\,\text{kg/s}$ (air at standard conditions).
- **Compressor Requirements:**
  - **Inlet total (stagnation) conditions:** $P_{01} = 100\,\text{kPa}$, $T_{01} = 300\,\text{K}$.
  - The compressor must achieve an overall pressure ratio of 3.3.
  - Assume the compressor stage is designed with a constant axial velocity and that ideal velocity triangle analysis applies.
- **Turbine Requirements:**
  - The turbine stage must be designed to extract sufficient work to drive the compressor.
  - Assume the turbine operates on the hot gases leaving a combustor with a total temperature $T_{03} = 1155\,\text{K}$ (after fuel addition) while maintaining a similar mass flow rate.

  - The turbine design should ensure that the net work extracted compensates for the compressor work demand while accounting for aerodynamic losses.

Design Tasks

Task 1: Compressor Stage Preliminary Design

1. Velocity Triangle Analysis

- Determine the axial and tangential velocity components at the inlet and exit of the compressor stage given:
  - A design inlet absolute velocity V_1 (choose a realistic value, e.g., around 150–250 m/s) and an inlet flow angle (e.g., 10°–15°).
  - An assumed design for constant axial velocity V_x throughout the compressor.
- Construct the inlet and outlet velocity triangles and estimate the change in relative velocities.

2. Pressure Rise Estimation

- Using the energy equation and the velocity triangle relations, derive an expression for the pressure rise per unit mass (as related to the enthalpy change) across the compressor stage.
- Incorporate an efficiency factor (e.g., assume a stage isentropic efficiency of about 80–85%) to estimate the actual pressure rise. Show detailed calculations and assumptions.

3. Design Discussion

- Briefly justify how the chosen inlet conditions, blade angles, and velocity components affect the compressor's performance.
- Discuss potential losses (such as profile and incidence losses) and how these can be minimized through blade design adjustments.

Task 2: Turbine Stage Preliminary Design

1. Work Matching and Energy Balance

- Estimate the compressor work requirement from Task 1 (expressed in kJ/kg).

- Establish the turbine work requirement, taking into account that the turbine must drive the compressor (assume mechanical coupling efficiency of about 95% if desired).

2. Velocity Triangle Analysis for Turbine

- Assume a turbine inlet absolute velocity V_{11} (typically higher than in the compressor; a starting value might be 300–400 m/s) and a design inlet flow angle (e.g., 25°–30°).
- Apply the free vortex or radial equilibrium assumption to design the turbine stage over a given radial range (for example, hub radius r_h and tip radius r_t can be specified or assumed).
- Construct detailed velocity triangles at the turbine inlet and exit. Compute the axial and tangential velocity components and derive the stage work contribution.
- Determine the necessary degree of reaction for the turbine stage and discuss its influence on the blade loading and efficiency.

3. Temperature Drop and Efficiency Considerations

- With the turbine inlet temperature $T_{03} = 1155\,\mathrm{K}$ and an assumed exit temperature based on the work extraction, calculate the total enthalpy drop (use the approximation $\Delta h_0 \approx c_p \Delta T_0$ with appropriate air properties).
- Adjust the work output by incorporating a correction for kinetic energy differences (suggest a typical loss fraction of 10–15%).

Task 3: Integrated System Analysis and Trade-offs

1. Matching Turbine to Compressor

- Summarize your compressor work requirement and compare it to the turbine work produced. Discuss how well the design is matched.
- If there is a disparity, describe design adjustments (e.g., altering blade angles, change in reaction degree, or adjusting the velocity components) that could better balance the two machines.

2. Sensitivity and Trade-off Analysis

- Discuss the trade-offs in selecting design parameters such as blade angles, and reaction degree.

- How would small deviations in flow assumptions affect the overall performance of the engine?
- Identify the main losses anticipated in both stages.

3. Documentation and Design Report

- Provide sketches of the velocity triangles, conceptual blade profiles, and schematic diagrams of the integrated system.
- Include all numerical results, derivations, and discuss any assumptions made.

Chapter 4

Solution Implementation

4.1 Compressor Stage Preliminary Design

4.1.1 Velocity Triangle Analysis

Inlet absolute velocity = V_1= 163 ms^{-1}
Inlet blade angle = α_1=13^o
Assumption= Constant axial velocity throughout the compressor
The normal and tangential components of velocity are defined as:

$$V_{1x} = V_1 cos(\alpha_1) \tag{4.1}$$

$$V_{1u} = V_1 sin(\alpha_1) \tag{4.2}$$

$$V_{1x} = 163 cos(13)$$

$$V_{1u} = 163 sin(13)$$

$$\boxed{V_{1x} = 158.82 \text{ ms}^{-1}}$$

$$\boxed{V_{1u} = 36.66 \text{ ms}^{-1}}$$

The reaction of compressor defined as the ratio of the change in static pressure in the rotating blades of a compressor or turbine, to the static pressure change in the compressor or turbine stage. For a compressor with reaction $R = 50\%$, the equation can be written as:

$$R = 1 - \frac{V_{u2} - V_{u1}}{2U} \tag{4.3}$$

The value of V_{u2} can be evaluated from following expression as

$$V_{u2} = U - V_{u1}$$

Where U is the blade speed. For typical axial compressors, the value of blade speed is between $250ms^{-1}$ and $350ms^{-1}$. **Since the blade speed is not given here, in reference to [23], the value of blade velocity has been taken as $U = 301ms^{-1}$.**

$$V_{u2} = 301 - 36.66$$

$$\boxed{V_{u2} = 264.34\ ms^{-1}}$$

The relative velocity at inlet can be computed using following equation:

$$|W_1| = \sqrt{(V_x)^2 + (U - V_{u1})^2} \tag{4.4}$$

$$|W_1| = \sqrt{(158.82)^2 + (264.34)^2}$$

$$\boxed{W_1 \approx 308.33\ ms^{-1}}$$

The relative flow angle at inlet (β_1) can be evaluated as:

$$\beta_1 = tan^{-1}(\frac{V_x}{U - V_{u1}}) \tag{4.5}$$

$$\beta = tan^{-1}(\frac{158.82}{264.34})$$

$$\boxed{\beta_1 = 30.998^o}$$

Similarly, the relative velocity at the outlet can be evaluated using following formula:

$$|W_2| = \sqrt{(V_x)^2 + (U - V_{u2})^2} \tag{4.6}$$

$$|W_2| = \sqrt{(158.82)^2 + (301 - 264.34)^2}$$

$$\boxed{W_2 \approx 163.00\ ms^{-1}}$$

The relative flow angle at outlet (β_2) can be evaluated as:

$$\beta_2 = tan^{-1}(\frac{V_x}{U - V_{u2}}) \tag{4.7}$$

$$\beta_2 = tan^{-1}(\frac{158.82}{301 - 264.34})$$

$$\boxed{\beta_2 = 77.00^o}$$

Table 4.1: Variables Involved in analysis of 4.1.1

Nomenclature	Identifiers	Values	Units
Inlet Absolute Velocity	V_1	163	ms^{-1}
Inlet Blade Angle	α_1	13	^{o}
Inlet Absolute Axial Velocity	V_{1x}	158.82	ms^{-1}
Inlet Absolute Tangential Velocity	V_{1u}	158.82	ms^{-1}
Reaction of Compressor	R	0.50 (Assumed)	-
Blade velocity	U	301 [23]	ms^{-1}
Outlet Absolute Tangential Velocity	V_{2u}	264.34	ms^{-1}
Inlet Relative Velocity	$\|W_1\|$	308.33	ms^{-1}
Outlet Relative Velocity	$\|W_2\|$	163.00	ms^{-1}
Inlet Relative Angle	β_1	30.998	^{o}
Outlet Relative Angle	β_2	77.00	^{o}

The velocity triangles for relative and absolute velocity about the inlet and outlet have been evaluated using MATLAB for ease of analysis with the corresponding code available through A.

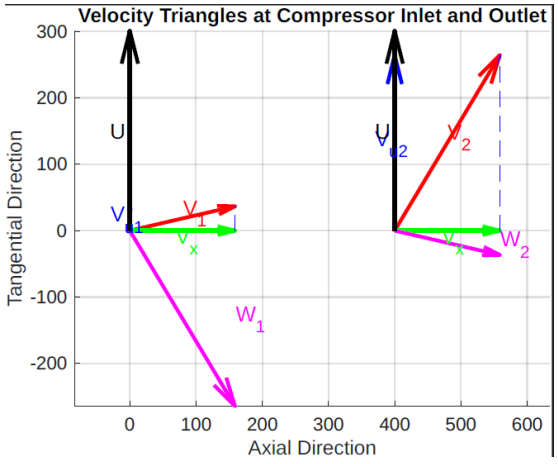


Figure 4.1: Velocity Triangles Evaluated at Inlet and Outlet of Compressor

4.1.2 Estimation of Pressure Rise

The specific work input to the fluid in a rotating machine is given by Euler's equation, which corresponds to the work input per unit mass:

$$\Delta W = U_2 V_{u2} - U_1 V_{u1}$$

where:

- U = blade speed at radius r ($U = \omega r$)
- V_u = tangential component of absolute velocity
- Subscripts 1 and 2 = inlet and outlet of rotor (relative to rotor)

Assuming steady state conditions, the thermodynamical balance can be applied such that:

$$\Delta h_0 = \Delta W$$

where h_0 is the stagnation enthalpy. Hence:

$$\Delta h_0 = U_2 V_{u2} - U_1 V_{u1}$$

The above expression relates the energy input to the velocity components. Considering a compressor for which the pressure rise per unit mass has to be evaluated. Corresponding to the thermodynamics, the enthalpy is the product of stagnation temperature and c_p, the specific heat capacity evaluated at constant pressure

$$\Delta h_0 = c_p \Delta T_0$$

Considering ideal gas behavior where

$$\Delta h_0 = \frac{\gamma}{\gamma - 1} \frac{R T_1}{p_1} \Delta p_0$$

Here

$$\gamma = \frac{c_p}{c_v}$$

is the ratio of specific heat capacity evaluated at constant pressure to specific heat capacity evaluated at constant volume. Neglecting energy changes (both kinetic and potential) across the entire compressor stage:

$$dh = v dp$$

where v is the specific volume of fixed amount of fluid (say gas). COnsidering incompressible fluid where changes are negligible

$$\Delta h \approx \frac{\Delta p}{\rho}$$

However, when one considers compressible flow, the relations require integration along some isentropic path or real-world constraints. The enthalpy rise directly corresponds to the pressure rise

As evaluated above:

$$\boxed{\Delta h_0 = U_2 V_{u2} - U_1 V_{u1}}$$

Enthalpy change acn be related with pressure change. For an isentropic process

$$\Delta h_0 = \int_{p_1}^{p_2} v \, dp$$

which can be simplified as:

$$\Delta h_0 = c_p (T_{02} - T_{01})$$

For incompressible fluid, the pressure rise per unit mass can be approximated as:

$$\Delta p = \rho \Delta h$$

However, for compressible fluid

$$\Delta p_0 = f(\Delta h_0)$$

Therefore, the pressure rise per unit mass is incorporated in Δh_0, while Δh_0 can be evaluated through velocity triangles and rotor speed corresponding to Euler's Turbomachinery Equation:

$$\boxed{\Delta h_0 = U_2 V_{u2} - U_1 V_{u1}}$$

while the pressure rise can be evaluated using thermodynamical relationships on the basis of assumptions taken into account.

The change in enthalpy can be evaluated using Euler's Equation of Turbomachinery as:

$$\Delta h = U(V_{u2} - V_{u1}) \tag{4.8}$$

$$\Delta h = 301(264.34 - 36.66)$$

$$\Delta h = 68531.68\ J/kg$$

$$\boxed{\Delta h = 68.531\ kJ/kg}$$

The above expression 4.1.2 gives the ideal enthalpy increase per unit mass.
The isentropic efficiency of the compressor used here is not provided. In general, the typical isentropic efficiency of an axial compressor is between $70\% - 85\%$. Thus, for sake of analysis, let $\eta_c = 0.83$.

$$\Delta h_{actual} = \frac{\Delta h}{\eta_c} \tag{4.9}$$

$$\Delta h = \frac{68.531}{0.83}$$

$$\boxed{\Delta h_{actual} = 82.5674\ kJ/kg}$$

The actual enthalpy achieved in a compressor can also be expressed in terms of stagnation temperature:

$$\Delta h_{actual} = c_p(T_{02} - T_{01}) \tag{4.10}$$

$$T_{02} = \frac{\Delta h_{actual}}{c_p} + T_{01}$$

$$T_{02} = \frac{82.5674}{1.005} + 300$$

$$\boxed{T_{02} = 382.1566\ K}$$

The pressure drop across an axial compressor can be expressed as:

$$(\frac{P_{02}}{P_{01}}) = (\frac{T_{02s}}{T_{01}})^{\frac{\gamma}{\gamma-1}} \tag{4.11}$$

The isentropic temperature of stagnation at outlet as T_{02s} can be evaluated as:

$$T_{02s} = T_{01}(\frac{P_{02}}{P_{01}})^{\frac{\gamma-1}{\gamma}}$$

For air, the value of γ is 1.4

$$\frac{\gamma - 1}{\gamma} = \frac{1.4 - 1}{1.4}$$

$$\boxed{\frac{\gamma-1}{\gamma} = 0.2857}$$

So,

$$T_{02s} = (300)(3.3)^{0.2857}$$

$$\boxed{T_{02s} = 421.949\ K}$$

In order to verify the calculation for pressure ratio, by substitution of outlet stagnation isentropic temperature in 4.11 equation to yield as:

$$(\frac{P_{02}}{P_{01}}) = (\frac{421.9}{300})^{\frac{1.4}{1.4-1}}$$

$$\boxed{\frac{P_{02}}{P_{01}} \approx 3.298 = 3.30}$$

which proves that the calculations are consistent. If one tries to evaluate the pressure difference using the actual outlet temperature T_{02}, then following expression can be used:

$$(\frac{P_{02}}{P_{01}}) = (\frac{T_{02}}{T_{01}})^{\frac{\gamma}{\gamma-1}} \tag{4.12}$$

$$(\frac{P_{02}}{P_{01}}) = (\frac{382.1566}{300})^{\frac{1.4}{0.4}}$$

$$\boxed{\frac{P_{02}}{P_{01}} \approx 2.333}$$

In that case the pressure ratio comes out to be 2.333. An important implication in

Table 4.2: Variables Involved in analysis of 4.1.2

Nomenclature	Identifiers	Values	Units
Enthalpy change	Δh	68.531	kJ/kg
Isentropic Compressor Efficiency	η_c	0.83	-
Actual Enthalpy change	Δh_{actual}	82.5674	kJ/kg
Inlet Stagnation Temperature	T_{02}	300	K
Outlet Stagnation Temperature	T_{03}	382.156	K
Ratio of specific heat capacity	γ	1.40	-
Isentropic Inlet Stagnation Temperature	T_{02s}	421.949	K
Stagnation Pressure Ratio	$\frac{P_{02}}{P_{01}}$	3.30	-
Actual Stagnation Pressure Ratio	$(\frac{P_{02}}{P_{01}})_{actual}$	2.33	-
Specific heat capacity of air	c_p	1.005	kJ/kg K

the performance of compressor is the extent of diffusion of fluid. Excessive diffusion corresponding to abrupt and sudden decrease in velocity with increase in pressure which can lead to boundary layer flow separation with the passage of time. In order to

restrict the excessive diffusion, De Haller's criterion comes into play which corresponds to performance of compressor given by follwoing expression:

$$\frac{W_2}{W_1} = \frac{cos(\beta_1)}{cos(\beta_2)} > 0.72 \tag{4.13}$$

For the very particular problem:

$$\frac{W_2}{W_1} = \frac{cos(\beta_1)}{cos(\beta_2)} = \frac{W_2}{W_1} = \frac{cos(30.998)}{cos(70)} = 3.8105 > 0.72$$

$$\boxed{\frac{W_2}{W_1} = \frac{cos(30.998)}{cos(70)} = 3.8105}$$

Since

$$3.8105 > 0.72$$

thus the compressor design is compatible The compressor flow coefficient can be evaluated using the following expression:

$$\phi = \frac{V_x}{U} \tag{4.14}$$

$$\phi = \frac{158.82}{301}$$

$$\boxed{\phi = 0.5276}$$

The following expression relates the work coefficient and flow coefficient of compressor in terms of relative inlet angle as:

$$tan\beta_1 = \frac{-R - \frac{\psi}{2}}{\phi} \tag{4.15}$$

Which can rearranged to evaluate the work coefficient as:

$$\psi = 2[-R - tan(\beta_1)\phi] \tag{4.16}$$

$$\psi = 2[-0.50 - tan(30.998)(0.5276)]$$

$$\boxed{\psi = 1.63}$$

The stagnation Mach number at compressor inlet is given by following expression:

$$M_{01} = \frac{V_x}{c_{01}} = \frac{V_x}{\sqrt{\gamma RT}} = \frac{163}{\sqrt{1.4 \times 287 \times 300}} = 0.4694 \tag{4.17}$$

$$\boxed{M_{01} = 0.4694}$$

4.1.3 Design Discussion 4.1

Impact of Inlet Velocity and Flow Angles on Incidence Losses

The inlet absolute velocity V_1 and flow angle at inlet α_1 play an important role in determining the angle of incidence i, which is the deviation in the flow direction and the blade inlet angle. Due to the mismatch between the adequate values of α_1 and β_1, incidence losses arise as the incoming flow tends to impinge on the blade at a non-optimal angle leading to flow separation and increased drag force which hinders optimal aerodynamical performance. Due to the influence of incidence, the fluid flow may experience high pressure gradient near the leading edge which may lead to flow separation from suction side and hence generating a leading-edge separation bubble, which in turn can cause total pressure recovery. Deviations from the optimal incidence angle by factor of ± 3 can lead to $20\% - 30\%$ more losses in high-speed axial compressors. Therefore, an adequate alignment between the values of α_1 and β_1 is necessary, especially during varying operation conditions. In order to mitigate the losses to some extent, variable inlet vanes can be used at part-load conditions.

Blade Loading and Fluid Flow Turning Limit

Blade loading refers to the amount of work made or extracted by the blade and the distribution of work about the length of blade from the hub to the tip/shroud. The typical aerodynamic behavior of turbomachinery is controlled predominantly by boundary layer effects [27]. The following figure shows the state of flow over an aerodynamical blade Blade loading highlights the pressure difference between the pressure and suction

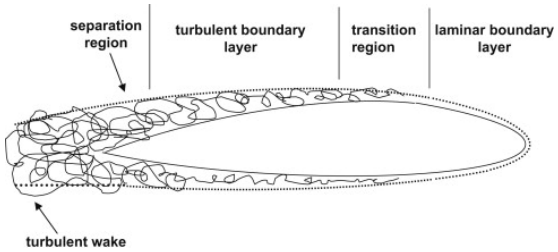


Figure 4.2: General state of the boundary layer flow over a turbomachine blade [27]

.

side of blade and is directly proportional to the velocity change i.e $V_{u2} - V_{u1}$ across the blade rotor. According to Euler's equation of turbomachinery as:

$$\Delta h = U(\Delta V_u)$$

By increasing the loading leads to greater energy transfer as flow tends to turn, hence greater the stage loading. Due to the increase in excessive flow turning, which corresponds to the deflection of flow between the inlet and outlet results in the increase in suction side curvature of blade which may lead to development of high pressure gradients, greater chances of boundary layer separation and larger wake regions. An important turbomachinery parameter, called Diffusion Parameter plays an important role in regulating the effects of flow separation and boundary layer separation. It is defined as:

$$D.F = 1 - \frac{V_2}{V_1} + \frac{\Delta V_u}{2V_1} \tag{4.18}$$

The value of diffusion factor should certainly be ≤ 0.6 in order to maintain optimum aerodynamic performance. According to [7] , it should be less than 0.4 for rotor tip and 0.6 for stator hub. In addition to aforementioned parameters, factors such as shock boundary-layer interaction and Mach number effects can also lead to boundary layer separation, which dominate under high loading conditions especially near the blade tips. Therefore, there should be an adequate balance to mitigate the effects from dominating. Blade loading should balance the work extraction and flow attachment and otherwise large values of ΔV_u can cater for increased stage work while putting the stability and efficiency losses at stake.

Strategies for Minimization of Profile and Secondary Flow Losses

While analyzing a compressor, the aerodynamic losses are categorized generally as;

- Profile Losses
- Secondary Losses

Profile Losses Profile losses are associated with the growth and separation of boundary and with wake formation along the blade surface.
Secondary Losses Secondary losses associated with the flow mechanics such as development of pressure gradients along the cross passage, tip leakage and corner vortices.
In order to minimize the profile losses, one may use CDA (Controlled Diffusion Aero foils) [26], which are specifically designed to cater for favorable pressure gradient along the entire suction side, thus delaying the effects of separation.Studies have suggested up to 30% reduction in profile losses by CDA blades as compared to conventional profiles under same loading conditions [16]. By the optimization of camber and thickness distribution of blade, the structural and aerodynamic demands can be effectively balanced and re-profiling of leading edge can cater for mitigation of sensitivity factor to the incidence angles. The secondary flow losses can be catered by designing the hub and casing walls in such a way to manipulate the boundary layer flow paths hence weakening the

secondary vortices and by filleting the blade-wall junction to certain degree can mitigate the vortex formation to a significant extent.By reducing space between blade tip and casing, tip leakages can be reduced significantly, primarily by designing the rotors without shrouds in low-pressure compressors to reduce leakage pathways and introduce tip seals.In order to sum up, one may deliberate over a high-performance compressor, which effectively integrates loss-reduction strategies, however there are certain implications. By using blades with high aspect ratio, flow turning can be increased at the cost of concentrated bending stress and thinner blades, while reduce the blockage are prone to mechanical failure with the passage of time due to high-pressure fluid flux. By contouring of region around end wall improves the efficiency but makes manufacturing difficult and adds on more cost.

The following figures show the cross-sectional view of compressor blade highlighting the major sections of blade. The blade schematics were visualized in MATLAB corresponding to which the code can be found as A and A.

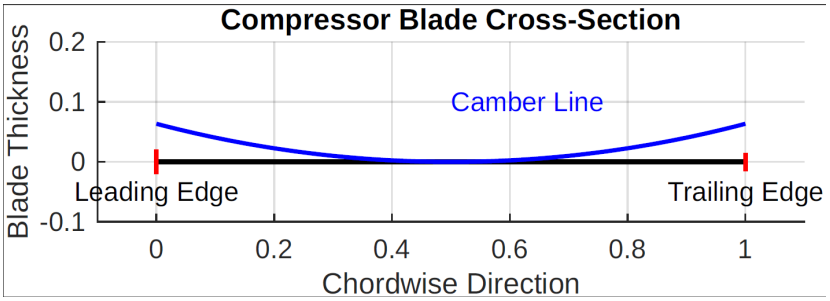


Figure 4.3: Compressor Blade Cross Section (Side View)

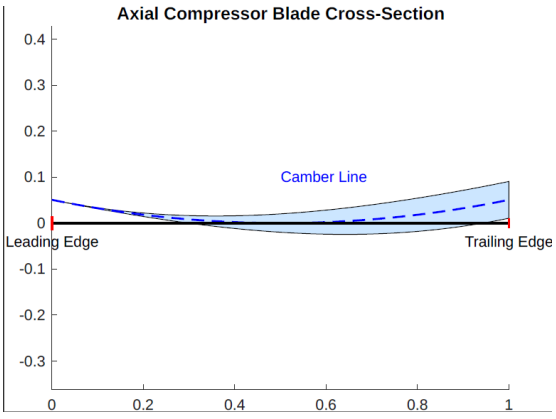


Figure 4.4: Compressor Blade Cross-Sectional Area

4.2 Turbine Stage Preliminary Design

4.2.1 Velocity Triangle Analysis

Referring to analysis on compressor work calculated in 4.1, the actual work done by the compressor for an isentropic efficiency of $\eta_c = 0.83$ was approximately 82.5674 kJ/kg.

$$\boxed{\Delta h_{actual_{compressor}} = W_{actual_{compressor}} = 82.5674\ kJ/kg}$$

Since the mechanical coupling efficiency range has been specified in the problem statement in 3, therefore an adequate value for mechanical coupling efficiency is taken as $\eta_m = 0.92$ The actual work done by turbine is given by following equation:

$$W_{turbine_{required}} = \frac{W_{actual_{compressor}}}{\eta_m} \tag{4.19}$$

$$W_{turbine_{required}} = \frac{82.5674}{0.92}$$

$$\boxed{W_{turbine} = 89.7472\ kW}$$

For further analysis let following parameters be taken into consideration: Turbine inlet absolute velocity $= V_{1t} = 345ms^{-1}$
Turbine inlet flow angle $= \alpha_{1t} = 29^o$
Assumption= Constant axial velocity throughout the turbine stage
Since the blade speed is not given here, in reference to [23], the value of blade velocity has been taken as $U = 301ms^{-1}$**.**

$$V_{x_t} = V_1 cos(\alpha_1)_t$$

$$V_{1u_t} = V_1 sin(\alpha_1)_t$$

$$V_{x_t} = 345cos(29)$$

$$V_{1u_t} = 345sin(29)$$

$$\boxed{V_{x_t} = 301.743\ \text{ms}^{-1}}$$

$$\boxed{V_{1u_t} = 167.260\ \text{ms}^{-1}}$$

From Euler's turbomachinery equation,

$$\Delta h = U(V_{u1_t} - V_{u2_t})$$

$$\frac{89747}{301} = 167.260 - V_{u2_t}$$

$$\boxed{V_{u2_t} = -130.9027\ ms^{-1}}$$

The negative sign of V_{u2t} indicates flow reversal in direction opposite to that of rotation (which implies that the blade swirl is opposite to the inlet swirl)

$$|W_1| = \sqrt{(V_x)^2 + (U - V_{u1_t})^2}$$

$$|W_1| = \sqrt{(301.743)^2 + (133.74)^2}$$

$$\boxed{W_1 = 330.053\ ms^{-1}}$$

The relative flow angle at inlet (β_1) can be evaluated as:

$$\beta_1 = tan^{-1}(\frac{V_x}{U - V_{u1}})$$

$$\beta = tan^{-1}(\frac{301.743}{133.74})$$

$$\boxed{\beta_1 = 66.095^o}$$

Similarly, the relative velocity at the outlet can be evaluated using following formula:

$$|W_2| = \sqrt{(V_x)^2 + (U - V_{u2_t})^2}$$

$$|W_2| = \sqrt{(301.743)^2 + (301 + 130.9027)^2}$$

$$\boxed{W_2 = 526.866\ ms^{-1}}$$

The relative flow angle at outlet (β_2) can be evaluated as:

$$\beta_2 = tan^{-1}(\frac{V_x}{U - V_{u2}})$$

$$\beta_2 = tan^{-1}(\frac{301.743}{301 + 130.9027})$$

$$\boxed{\beta_2 = 34.9395^o}$$

The velocity triangles at the turbine inlet and outlet corresponding to pre-defined parameters have been devised in MATLAB. The following figure shows the plots at the inlet and outlet while the code can be sourced in A

Table 4.3: Variables Involved in analysis of 4.2.1

Nomenclature	Identifiers	Values	Units
Turbine Inlet Absolute Velocity	V_{1t}	345	ms^{-1}
Turbine Inlet Blade Angle	α_{1t}	29	^{o}
Turbine Inlet Absolute Axial Velocity	V_{xt}	301.743	ms^{-1}
Turbine Inlet Absolute Tangential Velocity	V_{1ut}	167.260	ms^{-1}
Reaction of Compressor	R	0.9396	-
Blade velocity	U	301 [23]	ms^{-1}
Outlet Absolute Tangential Velocity	V_{2ut}	-130.902	ms^{-1}
Turbine Inlet Relative Velocity	$\|W_1\|$	320.053	ms^{-1}
Outlet Relative Velocity	$\|W_2\|$	526.886	ms^{-1}
Inlet Relative Angle	β_1	66.095	^{o}
Outlet Relative Angle	β_2	34.9395	^{o}
Enthalpy change	Δh	68.531	kJ/kg
Mechanical Coupling Efficiency	η_m	0.92	-
Actual Work by Compressor	$\Delta h_{actual,compressor}$	82.5674	kJ/kg
Work done by turbine	$\Delta h_{turbine}$	89.7472	kW

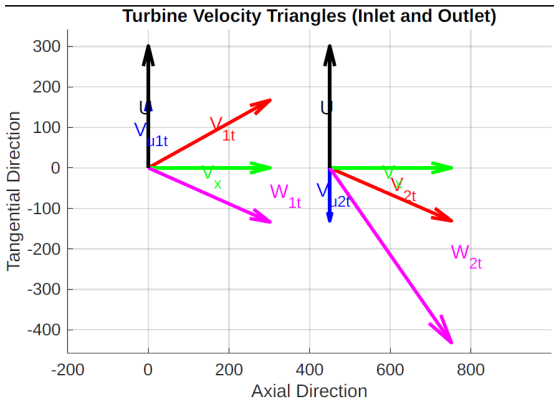


Figure 4.5: Turbine Velocity Triangles (Inlet and Outlet)

The following figure 4.6 shows the cross-sectional view of axial turbine cross-sectional area showing the leading and trailing edge with the chamber length taken as unit. The code corresponding to the development of cross-sectional area has been appended in A.

4.2.2 Application of Free Vortex Design to Turbine Stage

For general use turbines, the tangential component of velocity varies inversely with radius, a consequence of law of conservation of angular momentum and the radial pressure gradients. One common assumption made in turbomachinery design is the **free vortex law**, which ensures radial equilibrium without introduction of radial swirl gradients. Free vortex can be defined as the circular flow in a horizontal plane with no

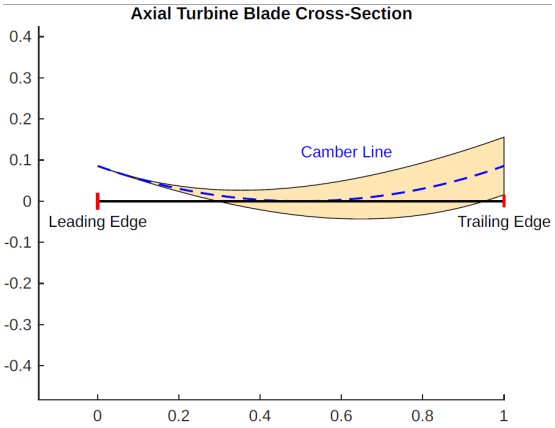


Figure 4.6: Axial Turbine Blade Cross-Section View

work done on the fluid. For free vortex, the velocity times the radius is a constant[25].

$$V_{u1_t} \times r = constant = k \tag{4.20}$$

The distribution of velocity about vortex is parabolic 4.7. From 4.20 equation, the

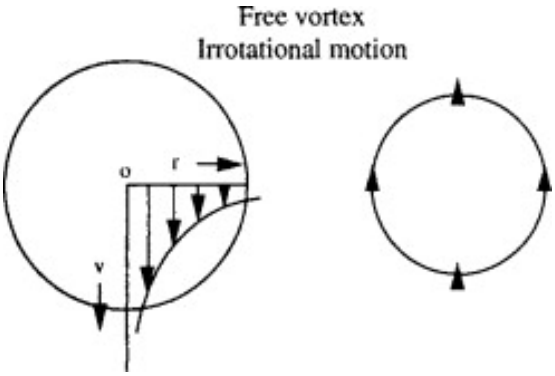


Figure 4.7: Free vortex rotational flow [25]

inverse relation between the tangential component of velocity and radius can be deliberated as

$$V_{u1_t} = \frac{k}{r} \tag{4.21}$$

The constant K can be evaluated using expression $V_{u1_t m} \times r_m$ where r_m is the mean radius, being the average of sum of hub radius r_h and tip radius r_t.
For the sake of analysis, let assumption be made as:
Hub Diameter = r_h=0.2 m
Tip Diameter = r_t=0.4 m

$$r_m = \frac{r_h + r_t}{2}$$

$$r_m = \frac{0.2 + 0.4}{2}$$

The mean radius r_m comes out to be 0.3 m. Since the tangential component of velocity evaluated at mean radius has been calculated previously such that

$$\boxed{V_{1u_t} = 167.260 \text{ ms}^{-1}}$$

thus

$$k = (167.260) \times (0.30)$$

$$k = 50.178 m^2 s^{-1}$$

The value of k comes out to be $50.178 m^2 s^{-1}$ In similar manner, the value of tangential velocity can be evaluated at the hub radius and tip radius using equation 4.2.2

$$V_{u1_t}(r_h) = \frac{k}{r_h} \tag{4.22}$$

$$V_{u1_t}(r_t) = \frac{k}{r_t} \tag{4.23}$$

$$V_{u1_t}(r_h) = \frac{50.178}{0.2}$$

$$\boxed{V_{u1_t}(r_h) = 250.89 \ ms^{-1}}$$

$$V_{u1_t}(r_t) = \frac{50.178}{0.4}$$

$$\boxed{V_{u1_t}(r_t) = 125.445 \ ms^{-1}}$$

The blade speed in general for any turbomachinery is given as:

$$U(r) = \Omega r \tag{4.24}$$

Where Ω is the angular speed in $rads^{-1}$ and r is the radius. Keeping in view the value of blade speed as $U = 301 ms^{-1}$ as from [23], the blade speeds at the hub and tip of blade can be calculated using following formulas:

$$U(r_h) = \Omega r_h \tag{4.25}$$

$$U(r_t) = \Omega r_t \tag{4.26}$$

where

$$\Omega = \frac{U}{r_m} = \frac{301}{0.3} = 1003.33 \ rads^{-1}$$

$$U(r_h) = (1003.33) \times (0.2)$$

$$\boxed{U(r_h) = 200.66\ ms^{-1}}$$

$$U(r_t) = (1003.33) \times (0.4)$$

$$\boxed{U(r_t) = 401.33\ ms^{-1}}$$

In order to evaluate the relative velocities and relative angles at the tip and hub of rotor following equations shall be used:

$$|W_1|_{t,h} = \sqrt{(V_x)_t^2 + (U_h - V_{u1_t,h})^2} \tag{4.27}$$

$$|W_1|_{t,t} = \sqrt{(V_x)_t^2 + (U_h - V_{u1_t,t})^2} \tag{4.28}$$

$$\beta_{1t,h} = tan^{-1}(\frac{V_{xt}}{U_h - V_{u1t,h}}) \tag{4.29}$$

$$\beta_{1t,t} = tan^{-1}(\frac{V_{xt}}{U_t - V_{u1t,t}}) \tag{4.30}$$

$$|W_1|_{t,h} = \sqrt{(301.743)^2 + (200.66 - 250.89)^2}$$

$$\boxed{W_{1t,h} = 305.895\ ms^{-1}}$$

$$|W_1|_{t,t} = \sqrt{(301.743)^2 + (401.33 - 125.445)^2}$$

$$\boxed{W_{1t,t} = 408.853\ ms^{-1}}$$

$$\beta_{1t,h} = tan^{-1}(\frac{301.743}{200.66 - 250.89})$$

$$\boxed{\beta_{1t,h} = -80.5488^o}$$

$$\beta_{1t,t} = tan^{-1}(\frac{301.743}{401.33 - 125.445})$$

$$\boxed{\beta_{1t,t} = 47.563^o}$$

In order to analyze the velocity triangles corresponding to each hub, rotor and mean radius, MATLAB code was implemented, aimed at overlaying the plot. The following figure depicts the overlayed plots and corresponding code as A.

From the above results, it can be implied that for relatively high swirling about hub

Table 4.4: Variables Involved in analysis of 4.2

Nomenclature	Identifiers	Values	Units
Mean radius	r_m	0.3	m
Hub radius	r_h	0.2	m
Tip radius	r_t	0.4	m
Free Vortex Constant	k	50.178	m^2s^{-1}
Tangential velocity at hub inlet	$V_{u1t}(r_h)$	250.89	ms^{-1}
Tangential velocity at tip inlet	$V_{u1t}(r_t)$	125.445	ms^{-1}
Angular speed of blade	Ω	1003.33	$rads^{-1}$
Blade velocity at hub	$U(r_h)$	200.66 [23]	ms^{-1}
Blade velocity at tip	$U(r_t)$	401.33 [23]	ms^{-1}
Turbine Inlet Relative Velocity at hub	$\|W_1\|_{t,h}$	305.895	ms^{-1}
Turbine Inlet Relative Velocity at tip	$\|W_1\|_{t,t}$	408.853	ms^{-1}
Inlet Relative Angle at hub	$\beta_{1,h}$	-80.5488	^{o}
Inlet Relative Angle at tip	$\beta_{1,t}$	47.563	^{o}

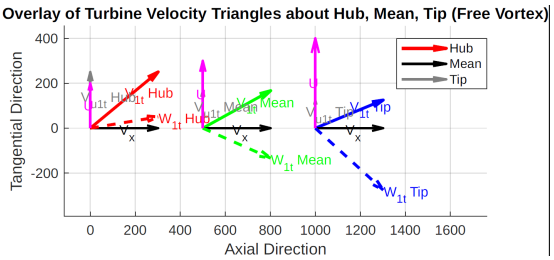


Figure 4.8: Overlaying of Velocity Triangles about the Rotor, Hub and Mean Radius

leads to a negative relative angle highlighting the flow reversal about the hub radius, something which is highly unfavorable. However, the analysis about tip resulted in positive relative angle, thus highlighting proper alignment with the flow. It is necessary to mention that the free vortex design tends to concentrates swirl towards the hub, which is suitable for reaction turbines, however it may require redistribution of vortex for uniform and effective blade loading. Increased tangential component about the hub indicates high loading which may suggest flow separation or stalling, which is indeed an unfavorable phenomenon and lead to decrease in efficiency, whereas lower tangential component of velocity about tip suggests reduced loading, a favorable consequence.

4.2.3 Reaction of Turbine

The reaction for a turbine can be calculated using following formula:

$$R = 1 - \frac{V_{u1_t} + V_{u2_t}}{2U} \tag{4.31}$$

$$R = 1 - \frac{167.260 - 130.9027}{2(301)}$$

$$R = 0.9396$$

A reaction value of $R = 0.9396$ is fairly a large value indicating that most of energy has been extracted in the rotor itself. It may be pertained that greater the reaction indicates greater rotor loading, which further indicates that the stator does not contribute much in the stage. in order to compensate for mechanical and thermal loading, adequate adjustments have to be made in blade profiles. Strong swirls tends to initiate at the exit of turbine which must be diffused or subsequently recovered in later stages.

4.2.4 Evaluation of Temperature Drop and Efficiency Considerations

The stagnation temperature at the inlet of temperature $T_{03} = 1155\ K$ has been specified for solution. The stagnation enthalpy about turbine can be evaluated suing following equation:

$$\Delta h_{0,turbine} = c_p(T_{03} - T_{04}) \tag{4.32}$$

Since the stagnation temperature at the inlet of turbine is $T_{03} = 1155\ K$, hence the specific heat capacity of air at said temperature is approximately 1168 J/kg K. Thus the stagnation temperature at outlet of turbine shall be evaluated using following formula:

$$T_{04} = T_{03} - \frac{\Delta h_{turbine}}{c_p} \tag{4.33}$$

$$T_{04} = 1155 - \frac{897472}{1168}$$

$$\boxed{T_{04} = 1078.16\ K}$$

Since the kinetic energy losses are not mentioned here, thus the most optimum value for kinetic energy losses can be chosen as $M_{loss} \sim 14.25\%$ The usable enthalpy corresponding to the kinetic energy losses can be evaluated as:

$$\Delta h_{usable} = (1 - M_{loss})\Delta h_{turbine} \tag{4.34}$$

$$\Delta h_{usable} = (1 - 0.1425)(89.747)$$

$$\boxed{\Delta h_{usable} = 76.9580\ kW}$$

Accounting for mechanical losses, it reduces the effective work done.

Table 4.5: Variables Involved in analysis of 4.2.3, 4.2.4

Nomenclature	Identifiers	Values	Units
Reaction of Turbine	R	0.9396	-
Work done by turbine	$\Delta h_{turbine}$	89.7472	kW
Inlet Stagnation Temperature	T_{03}	1155	K
Outlet Stagnation Temperature	T_{04}	1078.16	K
Kinetic Energy Losses	M_{loss}	0.1425	-
Usable work done	Δh_{usable}	76.9580	kW

4.3 Integrated System Analysis and Trade Offs

4.3.1 Matching of Performance by Turbine and Compressor

The performance of any turbomachine is governed effectively by maintaining an adequate balance between the work produced by a turbine and the work consumed by a compressor, compensated by inevitable mechanical and thermodynamic losses. Keeping in view the analysis performed in 4.1 and 4.2, the compressor was designed such to produce work output of

$$\boxed{\Delta h_{actual} = 82.5674\ kJ/kg}$$

. Accounting for the mechanical coupling efficiency of $\eta_m = 0.92$, the turbine should be capable of delivering work of approximately

$$\boxed{W_{turbine} = 89.7472\ kW}$$

Compensating for the kinetic energy losses within a turbine of approximately $M_{loss} = 14.25\%$, the usable work was calculated as

$$\boxed{\Delta h_{usable} = 76.9580\ kW}$$

This indicates work deficit of approximately $12.6094kW$, relative to the required compressor work. It is necessary to mention that from the above results, the current design assumptions are not compatible for the turbine to effectively meet the mechanical demands of compressor, thus leading to insufficient power transmission in order to maintain the cycle. This imbalance can affect the steady-state operation, significantly affect the pressure ratio or require providing extra energy to meet demands. It can also lead ro reduced mass flow capability, t=risking the compressor to stall. In practicality, the energy extraction capability of a turbine is limited significantly by aerodynamic loading, blade speed constraints and loss mechanism. An effective way of compensating the loss is either by increasing the turbine work or decreasing the compressor work

or manipulated in such a way that an adequate adjustment is made. There are certain design adjustments which can be made to improve the matching, which are discussed as follows:

- Increasing of blade speed U
- Increasing the Flow Turning $(V_{u1} - V_{u2})$
- Reducing the Reaction factor R
- Addition of extra turbine stage
- Reducing Loss Factors

Increasing the blade speed U

Increasing the blade speed is one way of compensating for shortfall in turbine work. According to the Euler's Equation for Turbomachinery:

$$\boxed{\Delta h = U(V_{u1_t} - V_{u2_t})}$$

An increase in blade speed shall result in greater work extraction. However, the increased blade speed leads to induction of mecahnical stresses within the blade as the centrifugal stress varies directly with the U^2, which could affect the durability and higher blade speed tends to push the tip Mach number towards transonic/supersonic regime, therefore introducing shock and wave drag and greater blade speed enhances tip leakage. Therefore, the increase in blade speed should be balanced by material strength, cooling capability and aerodynamical losses at high speeds.

Increasing the Flow Turning $(V_{u1} - V_{u2})$

By increasing the difference between the flow turning leads to an increase in work extraction, This can be achieved either by increasing the stator vane inlet speed V_{u1} or deceasing the exit speed V_{u2} by enhanced rotor turning. However, an increase in flow turning increases the diffusion factor which may encourage flow separation and higher incidence about rotor inlet significantly increases the stalling sensitivity and reduced blade efficiency.

Decreasing the Reaction Degree of Turbine (R)

The current turbine design operates with reaction value of $R = 0.9396$ is fairly a large value indicating that most of energy has been extracted in the rotor itself. It may be pertained that greater the reaction indicates greater rotor loading, which further

indicates that the stator does not contribute much in the stage. By reducing the reaction degree shifts the enthalpy extraction about the rotor and increase in flow turning shall result in greater work extract according to Euler's Equation of Turbomachinery and it shall also reduce the rotor loading thereby requiring lesser blade speed for effective work extraction. However, it is important to mention that decreasing the reaction degree will require stronger stator turning which in turn shall result in higher incidence loss about stator and it also affects the downstream velocity triangle by introducing mismatch in rotor.

Addition of Extra Turbine Stage

The addition of extra turbine stage is deemed necessary when work extraction is not feasible through single stage without overloading, then an optimum way of improving work extraction is by adding an additional turbine stage, which shall allow for enthalpy drop effectively about individual stage. For lesser flow turning shall result in lesser diffusion thereby greater efficiency. However, the addition of extra stage leads to mechanical complexity and larger length. Multi-stage turbines are used in aeronautical applications with above trade-offs taken into account.

Reduction of Loss Factor

Considering the design of this turbine, mechanical losses were kept $\approx 14.25\%$. Reduction in mechanical losses recovers the enthalpy drop into useful work with improving exhaust velocity recovery (via optimized diffuser) can significantly reduce the effective energy lost, thereby increasing usable turbine work without altering the core thermodynamic cycle.

Conclusion

In conclusion, the current design shows power imbalance which can be compensated through many different methodologies as discussed above. The redistribution of enthalpy extraction between the stator and rotor can be achieved by reducing the reaction degree. by higher flow turning or increasing the blade speed, yet at the cost of mechanical failure also increases the work deficit. IN addition to that, the consideration of multi-stage turbine can be considered for mitigating work deficit by effectively distribution enthalpy drop about each stage

4.3.2 Sensitivity and Trade-Off Analysis

Trade Offs in Blade Angle Selection

The choice of optimum blade angle greatly affects the efficiency of turbomachine. Factors such as incidence loss, flow turning capability and mechanical feasibility are governed by adequate choice of blade angles. For relatively small values of inlet angle α_1 results in flow misalignment which in turn, enhances flow separation, thereby increasing the stagnation pressure loss. Considering the flow turning capability, increasing the turning factor leads to an increase in flow turning which does improve the work output. However, increased flow turning leads to enhancement in influence of aerodynamical losses such as flow separation, tip leakages which greatly affect the performance of machine. Considering greater values of blade angles demand more robust and rigid structures capable of sustaining extreme conditions within the machine and increased blade chord length to maintain the loading limits.

- Keeping in the blade angles, a deviation of $\pm 2^o - 3^o$ in α_1, β_1 can result in increased incidence losses by factor of $15\% - 30\%$ depending on the loading factor
- An off-design in blade construction by factor of $\pm 5^o$ can increase the stalling by approximately 10% while pushing the compressor towards major surge
- Misalignment within rotor blade design significantly increases the tip leakage, thereby affecting the loss coefficient by factor of 2% *to* 5% per degree increase in high-loaded blade designs.

Trade Offs in Reaction Degree

The reaction degree R of turbomachinery plays an important role in signifying the enthalpy division between the stator and rotor. For relatively high vales of reaction, the rotor speed sensitivity decreases and so does the stator pressure ratio contribution. High reaction of turbine means greater the work extraction which can induce mechanical stresses on blades reducing the efficiency in long run. For relatively less values of reaction, the work extraction is dependent more on stator than rotor while the sensitivity to upstream flow condition increases significantly. With lesser degree of reaction, the stator flow turning requirement increases leading to more stator losses. Thus the most optimum choice of R should be such to balance the mechanical loading, flow acceleration and downstream pressure recover.

Sensitivity to Flow Assumptions

Turbomachinery, regardless of sub-types are highly sensitive to flow variables. Small variations lead to significant impact on overall performance of machine in long-run.

Considering the inlet angles, α_1, β_1, a deviation by factor of $\pm 3^o$ can lead to increased incidence losses by factor of 15% to 30% which in turn reduces the stage efficiency. Considering the mass flow rate, a change by factor of $\approx$ 5% can lead to surging or choking within a compressor, which gretaly affects the pressure ratio downstream and the operating line. Considering the turbine, the inlet stagnation temperature T_{03} when varied by factor, say $\pm 10\ K$ can result in enthalpy drop thsus reducing the available turbine work by factor of 1 kJ/kg per 10 K, as

$$\boxed{\Delta W_t \approx c_p \Delta T \approx 1005 \times 10 = 10.05\ kJ/kg}$$

which signifies the comparability to current work deficit highlighting the dependence on the inlet temperature. For gas turbines, the temperature and mass flow stability serve as fundamental parameters in matching the most optimum mechanical balance.

4.3.3 Anticipated Losses within Compressor and Turbine Stages

On broader perspective, aerodynamic losses dominate within the compressor and turbine stages leading to a consequent decrease in optimal performance and efficiency of turbomachinery. Following are some important aerodynamical losses within turbines and compressors

Compressor

- Incidence Losses
- Profile Losses
- Secondary Flow Loss
- Tip Leakage

Turbine

- Tip Leakage
- Secondary Losses
- Trailing Edge Losses
- Exit Kinetic Energy Loss

Incidence Losses

Incidence losses generally arise from misalignment of incoming flow with the leading edge of turbomachine's blade (which corresponds to misaligned α_1, β_1deviating from the design). Such misalignment, as discussed above, can lead to flow separation about the leading edge leading to formation of stagnation zones and hence increased total pressure loss. In order to mitigate such incidence losses, following strageties can be taken into account:

- Variable Inlet guide Vanes (VIGVs): VIGVs are extensively used in centrifugal compressors, commonly used to adjust the airflow and improve performance. they tend to change the angle of incoming flow, thus optimizing the compressor's efficiency and expand the operating range [4].
- Re-profiling about Leading Edge: By re-profiling, it means filleting the region about the endwalls of turbomachine which helps to reduce the extent of separation at the incidence.
- Blade Stacking ans Sweeping: The 3D blades of turbomachinery can be shaped accordingly to redistribute the incidence along the entire span of blade, thereby improving the tolerance.
- Active Flow Control (AFM jets): The use of small perturbations about the flow field to minimize the aerodynamical phenomenon such as flow separation, thereby improving overall performance. The aerodynamic performance can be enhanced by reducing adverse effects of separated flow, potentially improving efficiency and reducing drag [18],[13].

Profile Losses

Profile losses generally arise from the viscous boundary layer growth along the surfaces of blade, which leads to a significant increase in drag, which in turn influences the momentum deficit in wake behind the blade, which in turn, contributes to stagnation pressure loss. The profile losses generally increase with the surface roughness, increasing boundary layer thickness and development of adverse pressure gradients. In order to mitigate profile losses , following strategies can be taken into account.

- The use of low-loss aerofoils such as Controlled Diffusion Aerfoils [26] or NACA 65-series, these contribute to lesser losses, and lead to controlled diffusion blades best optimized for low drag coefficient.
- Using polished or adequately coated blade surfaces reduce the surface roughness factor, hence lesser skin friction

- Boundary layer separation has to be controlled along the suction side of blade profile to reduce aerodynamic losses
- The optimization of Reynolds number can play a huge role in minimizing profile losses, the choice of Re should be such that the flow remains within the favorable region in order to avoid lamiinar separation

Secondary Flow Losses

Secondary flow losses generally arise from the 3D flow affects in the blade passage, mainly due to adverse pressure gradients at the suction side across blades near the end walls. These secondary loses lead to formation of horseshoe vortices about the leading edge or the hub casing with the pressure vortices moving towards the mid-span of blase. The consequence is cross-passage pressure driven flows. Horseshoe vortices lead to an increase in loss coefficient and disturb the exit flow angles, thus affecting the downstream stages. In order to cater for secondary losses, following strategies can be taken into account:

- By contouring or filleting the endwalls about the ends help to counter the adverse pressure gradient driving secondary flows and using flow control devices such as vortex brakes, being placed at the endwalls to cater for the dampening of vortices being formed.
- By adjusting the loading distribution about the blade lean and sweep plays an important role in weakening the cross-flow drivers.
- By making the blades more curved (like in the shape of a bow) lead to redistribution of loading in radial direction helps to weaken the vortices being generated.

Tip Leakage Losses

Tip Leakage losses arise in unshrouded turbomachinery blades due to pressure difference developed across blade tips leading to leakage flow over tip gaps, leading to formation of tip leakage vortices. Tip leakage losses lead to reduced effective turning of blades, which in turn lead to mixing of losses within the fluid flow and increased entropy generation. The extent of tip leakages increase with an increase in the tip clearance height, pressure ratio and extent of blade loading. In order to minimize the tip leakage losses, certain strategies can be adopted such as:

- Implementation of tip shorouds which tend to physically block the leakage path, yet it adds to the weight and stress within the machine.
- By using squealer tips, which are characterized by a raised rib along the tip

diameter, play an important role in reducing the tip leakage by increasing the resistance to the leakage flow. This resistance casues sealing effect which mitigates the flow of fluid across the blade tip gap [12],[6].

- Active Clearance Control (ACC): Active Clearance Control (ACC) is commonly implemented in gas turbines to reduce the tip leakage by adjusting the gap between blades of turbines and the casing during operation. ACC can be done either thermally of mechanically, respectively by cooling the air to shrink the casing or using actuators to move through the course of casing [22],[29].

Trailing Edge Losses

Trailing edge losses are generally associated with the mixing of low-momentum wake behind the blade trailing edge into the main flow leading to mixed entropy and stagnation pressure loss. The trailing edge losses increase with a thicker trailing edge, increased wake width and adverse pressure gradient established at the trailing edge The trailing edge losses can be minimized by adopting following strategies:

- By making the trailing edges thinner, the wake thickness decreases. However, the mechanical strength is not compromised and it is maintained.
- By aligning the wake with the flow direction, vortices tend to generate downstream
- One key way of minimizing the trailing edge losses is by optimization of trailing edge shape, by making it in the shape of a cusp or bevel, the pressure tends to distribute uniformly which can later be recovered, it leads to reduction in mixing entropy [20],[31],[19],[10].

Exit Kinetic Energy Loss

Exit kinetic energy loss correspinds to the residual kinetic energy left in a flow about the turbine exit, which is not converted to useful work. Exit kinetic energy loss is expressed in terms of exhaust velocity and corresponds to exergy lost. Mathematically,

$$KE_{exit} = \frac{v_{exit}^2}{2} \tag{4.35}$$

The kinetic energy is usually lost unless recovered by the diffuser or some downstream system. Following are some important mitigation strategies which can be taken into account for minimizing the exite kinetic energy losses:

- Using an exhaust diffuser downstream turbine whihc aims at converting the dynamic pressure into static pressure thus leading to recovery in usable pressure

- Designing of blades such to minimize the swirl about the exit, which implies the reduction of residual tangential velocity achievable by lowering the exit kinetic energy.
- By using a multistage turbine, the enthalpy can be evenly distributed among stages and it aims at avoiding high per-stage velocity drops.

4.4 Assumptions Considered for Effective Analysis

4.4.1 General Thermodynamic and Fluid Assumptions

Blade Speed

The blade speed was not provided, hence according to [23], the value was taken as $U = 301 ms^{-1}$.

Ideal Behavior of Air

Air was considered as an ideal gas with the value of c_p taken as 1005 J/kgK. This assumption is generally valid till temperature range of 1200 K. Due to this assumption, the enthalpy drop about stagnation temperature of turbine inlet as $T_{03} = 1155$ K may be underestimated.

Negligible heat transfer about Compressor and Turbine Blades

Adiabatic flow was assumed about the compressor and turbine blades, which corresponds to no heat loss or gain to the surroundings.

No Distortion

No inlet distortion about compressor inlet were considered, while assuming perfectly uniform, axial flow entering the compressor.

Coupling Efficiency

Overall mechanical coupling efficiency was considered $\eta_m = 0.92$. The mechanical losses may be underestimated in complex engine configurations

Quasi-One Dimensional Flow

No radial pressure gradients except for free vortex in turbine were considered. The pressure variation about the compressor was ignored which further accounts for radial variation in turbine using free-vortex assumption.

4.4.2 Compressor Design Assumptions

Constant Axial Velocity

In designing of compressor, constant axial velocity across the compressor stage was taken into consideration, which assumes unchanged axial velocity from the inlet to rotor exit. In this assumption, the effects of diffusion or acceleration in axial velocity are neglected and validates fpr preliminary design however mot suitable for detailed path flow.

Inlet Absolute velocity

The inlet absolute velocity was considered as $V_1 = 163ms^{-1}$ with flow angle $\alpha_1 = 13^o$. the choice was made based on subsonic axial compressor design range.

Fixed Compressor Pressure Ratio

The compressor pressure ratio was fixed at 3.3 throughout the analysis, corresponding to which all the velocity triangles and stage loadings meet the target.

Single-Stage Equivalence

For the sake of ease in analysis, the compressor was designed for single stage hence representing the net performance. In practical world, the stage loading per stage is reduced in real engine with actual multi-stage compressor may distribute work in different manner.

4.4.3 Turbine Design Assumptions

Inlet Stagnation Temperature

The inlet turbine stagnation temperature was taken as $T_{03} = 1155\ K$ which is representative of low to intermediate temperature turbine requiring no extensive cooling.

Free Vortex Design for Radial Equilibrium

The tangential component of velocity varies inversely with the radius, which simplifies the 3D velocity field by ignoring the spanwise loading or non-vortex designs.

$\approx 93\%$ Reaction

The stage-reaction degree was assumed and evaluated as $\approx 93\%$ which corresponds to the fact that high reaction increases rotor loading while reducing the stator work contribution.

Losses in Kinetic Energy

The losses in kinetic energy were assumed to be approximately 14.25% which was later used as correction factor on output work.

Neglecting of Cooling Air

the cooling air mass flow bleed and mixing losses were ignored while assuming entire mass flow being available for work extraction. In real turbines, some fraction of flow rate is lost for cooling.

Single Stage Analysis

The turbine was modeled as single-stage for matching, by omitting multi-stage expansion, which however limits the achievable enthalpy drop per stage.

4.4.4 Integrated System Assumptions

Fixed Mechanical Coupling Efficiency

The mechanical coupling efficiency was fixed at $|eta_m = 0.92$ which is typical for small engines, however large engines tend to have different values depending on the accessory system.

No Surge

No surge or choking was susceptible with the analysis being conducted at design point without margin evaluation

Negligible impact of Fuel Addition

The mass flow rate of fuel as $\dot{m}_{fuel}$ was considered negligible as compared to the $\dot{m}_{air}$

Ambient Conditions

Throughout the entire analysis, ambient air conditions were taken into account, with the c_p remaining 1005 J/kgK or 1.005 kJ/kgK.

4.5 Integrated System Design

The following figures shows the schematic of engine stage comprising of compressor and turbine with and without annotations. The schematics have been devised in MATLAB corresponding to which the code has been appended in A and A.

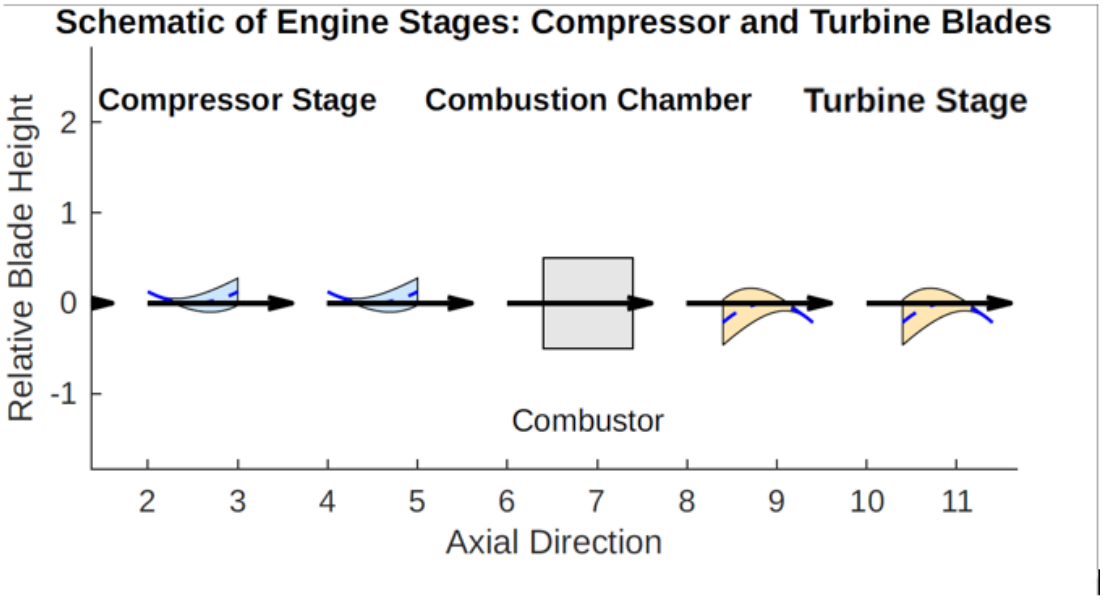


Figure 4.9: Schematic of Engine Stage: Compressor and Turbine

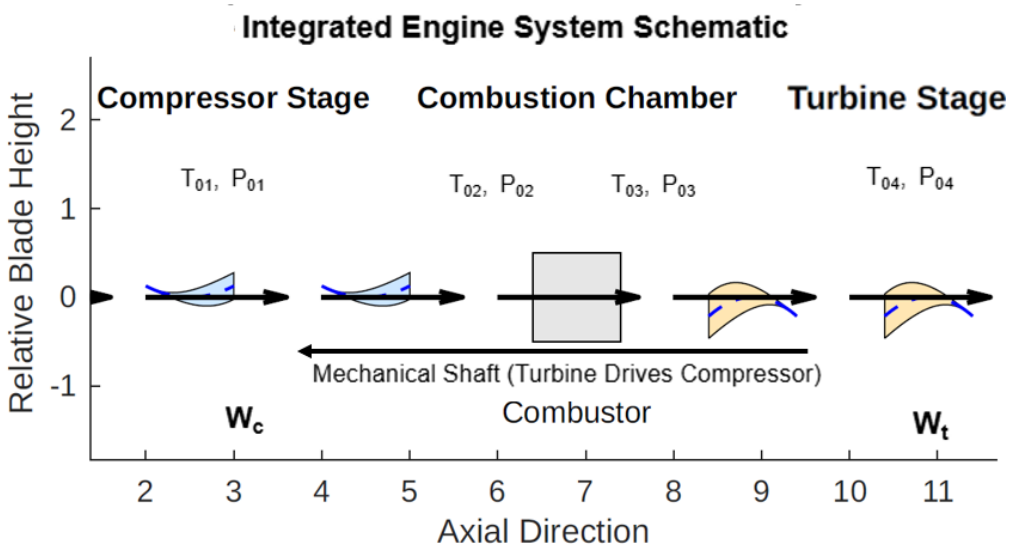


Figure 4.10: Integrated Engine System Schematic

Table 4.6: Cumulative Variables Involved in analysis of 4.1

Nomenclature	Identifiers	Values	Units
Inlet Absolute Velocity	V_1	163	ms^{-1}
Inlet Blade Angle	α_1	13	^{o}
Inlet Absolute Axial Velocity	V_{1x}	158.82	ms^{-1}
Inlet Absolute Tangential Velocity	V_{1u}	158.82	ms^{-1}
Reaction of Compressor	R	0.50 (Assumed)	-
Blade velocity	U	301 [23]	ms^{-1}
Outlet Absolute Tangential Velocity	V_{2u}	264.34	ms^{-1}
Inlet Relative Velocity	$\|W_1\|$	308.33	ms^{-1}
Outlet Relative Velocity	$\|W_2\|$	163.00	ms^{-1}
Inlet Relative Angle	β_1	30.998	^{o}
Outlet Relative Angle	β_2	77.00	^{o}
Enthalpy change	Δh	68.531	kJ/kg
Isentropic Compressor Efficiency	η_c	0.83	-
Actual Enthalpy change	Δh_{actual}	82.5674	kJ/kg
Inlet Stagnation Temperature	T_{02}	300	K
Outlet Stagnation Temperature	T_{03}	382.156	K
Ratio of specific heat capacity	γ	1.40	-
Isentropic Inlet Stagnation Temperature	T_{02s}	421.949	K
Stagnation Pressure Ratio	$\frac{P_{02}}{P_{01}}$	3.30	-
Actual Stagnation Pressure Ratio	$(\frac{P_{02}}{P_{01}})_{actual}$	2.33	-
Specific heat capacity of air	c_p	1.005	kJ/kg K
De Haller's Criterion	$\frac{cos(\beta_1)}{cos(\beta_2)}$	3.8105	-
Flow coefficient	ϕ	0.5276	-
Work coefficient	ψ	1.63	-
Inlet stagnation Mach number	M_{01}	0.4694	-

Table 4.7: Variables Involved in analysis of 4.2

Nomenclature	Identifiers	Values	Units
Turbine Inlet Absolute Velocity	V_{1t}	345	ms^{-1}
Turbine Inlet Blade Angle	α_{1t}	29	^{o}
Turbine Inlet Absolute Axial Velocity	V_{xt}	301.743	ms^{-1}
Turbine Inlet Absolute Tangential Velocity	V_{1ut}	167.260	ms^{-1}
Reaction of Turbine	R	0.9396	-
Blade velocity	U	301 [23]	ms^{-1}
Outlet Absolute Tangential Velocity	V_{2ut}	-130.902	ms^{-1}
Turbine Inlet Relative Velocity	$\|W_1\|$	320.053	ms^{-1}
Outlet Relative Velocity	$\|W_2\|$	526.886	ms^{-1}
Inlet Relative Angle	β_1	66.095	^{o}
Outlet Relative Angle	β_2	34.9395	^{o}
Enthalpy change	Δh	68.531	kJ/kg
Mechanical Coupling Efficiency	η_m	0.92	-
Actual Work by Compressor	$\Delta h_{actual,compressor}$	82.5674	kJ/kg
Work done by turbine	$\Delta h_{turbine}$	89.7472	kW
Inlet Stagnation Temperature	T_{03}	1155	K
Outlet Stagnation Temperature	T_{04}	1078.16	K
Kinetic Energy Losses	M_{loss}	0.1425	-
Usable work done	Δh_{usable}	76.9580	kW
Mean radius	r_m	0.3	m
Hub radius	r_h	0.2	m
Tip radius	r_t	0.4	m
Free Vortex Constant	k	50.178	m^2s^{-1}
Tangential velocity at hub inlet	$V_{u1t}(r_h)$	250.89	ms^{-1}
Tangential velocity at tip inlet	$V_{u1t}(r_t)$	125.445	ms^{-1}
Angular speed of blade	Ω	1003.33	$rads^{-1}$
Blade velocity at hub	$U(r_h)$	200.66 [23]	ms^{-1}
Blade velocity at tip	$U(r_t)$	401.33 [23]	ms^{-1}
Turbine Inlet Relative Velocity at hub	$\|W_1\|_{t,h}$	305.895	ms^{-1}
Turbine Inlet Relative Velocity at tip	$\|W_1\|_{t,t}$	408.853	ms^{-1}
Inlet Relative Angle at hub	$\beta_{1,h}$	-80.5488	^{o}
Inlet Relative Angle at tip	$\beta_{1,t}$	47.563	^{o}

Chapter 5

Conclusion

5.1 Conclusions

This research-driven project has successfully conducted a comprehensive preliminary design and analysis of a single-stage axial compressor and a matching turbine stage for a small gas turbine engine. By extensive literature review and implementing integrating methodology of combining the velocity triangle analysis, implementation of thermodynamic energy balance, and aerodynamic work correlations, the study highlights a thorough and deep understanding regarding the design principles behind turbomachinery and their practical implications. The compressor stage was designed to achieve a pressure ratio of 3.3 for mass flow rate of $0.74kg/s$, which led to an actual enthalpy rise of $82.56kJ/kg$ under an assumed isentropic efficiency of 83%. The turbine stage designed to produce sufficient work to drive the compressor while accounting for a mechanical coupling efficiency of 92% and kinetic energy losses of 14.25%, achieved a usable work output of $76.95kJ/kg$. During the analysis, work deficit of approximately $12.6kJ/kg$ was observed, which corresponded to a fundamental mismatch in turbine-compressor coupling under initial design conditions. The analysis critically identified the interaction of blade speed, flow turning, reaction degree, and stage loading in effectively balancing turbine work and compressor demand. A deep sensitivity analysis was conducted which shed light on minute deviations and discrepancies in blade angles, mass flow, and inlet temperatures can significantly impact performance, efficiency, and surge margins. In addition to that, the study highlighted some key aerodynamic losses—including incidence, profile, secondary flow, tip leakage, and trailing edge mixing losses—within both stages. For mitigation of such losses, techniques such as variable inlet guide vanes, controlled diffusion airfoils, endwall contouring, tip shrouds, and exhaust diffusers were suggested on the basis of initial research to cater for these losses.

5.2 Future Work

Corresponding to the preliminary compressor and turbine stage design, several work mismatch factors and limitations were identified. Some future directions for redressal of shortcomings are recommended as follows:

1. Incorporation of Multi-Stage Turbine Design: By the addition of an additional turbine stage, the enthalpy drop shall distribute more evenly through the stages, hence reduing the diffusion factor per stage and mitigating mechanical and aerodynamical loading per rotor.

2. Validation through Computational Fluid Dynamics (CFD) : While the current analysis was dependent on mean-line and 1D approximations, CFD simulations may be employed in future to effectively capture secondary flows, boundary layer development and propogation, and three-dimensional flow features critical to high-fidelity performance prediction.

3. Conducting of Structural and Thermal Stress Analysis: The mechanical integrity of blades under centrifugal loading and thermal gradients can be analyzed by simulations on *Ansys* or *Abacus*, predominantly if blade speed or turbine inlet temperature are increased to meet work balance.

4. Explore Advanced Blade Profiles and Cooling Strategies: High-efficiency modern blade profiles can be incorporated with enhanced film cooling design, and thermal barrier coatings to prolong the allowable operating temperature range without compromise on material limits.

5. Development of Off-Design Performance Maps: The analysis can be extended beyond design point to effectively incorporate the surge margin, choke margin, and part-load operation behavior to ensure robustness under varying operating conditions.

Bibliography

[1] T. Adefarati and R.C. Bansal. "Chapter 2 - Energizing Renewable Energy Systems and Distribution Generation". In: *Pathways to a Smarter Power System*. Ed. by Akın Taşcıkaraoğlu and Ozan Erdinç. Academic Press, 2019, pp. 29–65. ISBN: 978-0-08-102592-5. DOI: https://doi.org/10.1016/B978-0-08-102592-5.00002-8. URL: https://www.sciencedirect.com/science/article/pii/B9780081025925000028.

[2] T. Adefarati et al. "Non-Renewable Distributed Generation Technologies: A Review". In: *Handbook of Distributed Generation*. Springer, 2017, pp. 69–105.

[3] Falah Alobaid et al. "Progress in dynamic simulation of thermal power plants". In: *Progress in Energy and Combustion Science* 59 (2017), pp. 79–162. ISSN: 0360-1285. DOI: https://doi.org/10.1016/j.pecs.2016.11.001. URL: https://www.sciencedirect.com/science/article/pii/S0360128516300375.

[4] Ken Arnold and Maurice Stewart. "CHAPTER 10 - Compressors **Reviewed for the 1999 edition by John H. Galey of Paragon Engineering Services, Inc." In: *Surface Production Operations: Design of Gas-Handling Systems and Facilities (Second Edition)*. Ed. by Ken Arnold and Maurice Stewart. Second Edition. Woburn: Gulf Professional Publishing, 1999, pp. 253–285. ISBN: 978-0-88415-822-6. DOI: https://doi.org/10.1016/B978-088415822-6/50011-8. URL: https://www.sciencedirect.com/science/article/pii/B9780884158226500118.

[5] E. A. Baskharone. *Principles of Turbomachinery in Air-Breathing Engines*. Cambridge University Press, 2006, p. 580.

[6] Shuai Bi et al. "Effect of multiple cavities and tip injection on the aerothermal characteristics of the squealer tip in turbine stage". In: *Applied Thermal Engineering* 220 (2023), p. 119631. ISSN: 1359-4311. DOI: https://doi.org/10.1016/j.applthermaleng.2022.119631. URL: https://www.sciencedirect.com/science/article/pii/S1359431122015617.

[7] Meherwan P. Boyce. "7 - Axial-Flow Compressors". In: *Gas Turbine Engineering Handbook (Fourth Edition)*. Ed. by Meherwan P. Boyce. Fourth Edition. Oxford: Butterworth-Heinemann, 2012, pp. 303–355. ISBN: 978-0-12-383842-1. DOI:

https://doi.org/10.1016/B978-0-12-383842-1.00007-X. URL: https://www.sciencedirect.com/science/article/pii/B978012383842100007X.

[8] Paul Breeze. "Chapter 4 - Natural Gas–fired Gas Turbines and Combined Cycle Power Plants". In: *Power Generation Technologies (Second Edition)*. Ed. by Paul Breeze. Second Edition. Boston: Newnes, 2014, pp. 67–91. ISBN: 978-0-08-098330-1. DOI: https://doi.org/10.1016/B978-0-08-098330-1.00004-1. URL: https://www.sciencedirect.com/science/article/pii/B9780080983301000041.

[9] Yunus A. Çengel and John M. Cimbala. *Fluid Mechanics: Fundamentals and Applications*. McGraw-Hill Series in Mechanical Engineering. Boston, Mass.: McGraw-Hill Higher Education, 2006, p. 735. ISBN: 978-0-07-247236-3.

[10] Baoling Cui et al. "Influence of Cutting Angle of Blade Trailing Edge on Unsteady Flow in a Centrifugal Pump Under Off-Design Conditions". In: *Applied Sciences* 10.2 (2020). ISSN: 2076-3417. DOI: 10.3390/app10020580. URL: https://www.mdpi.com/2076-3417/10/2/580.

[11] S.L. Dixon and C.A. Hall. "Chapter 1 - Introduction: Basic Principles". In: *Fluid Mechanics and Thermodynamics of Turbomachinery (Seventh Edition)*. Ed. by S.L. Dixon and C.A. Hall. Seventh Edition. Boston: Butterworth-Heinemann, 2014, pp. 1–37. ISBN: 978-0-12-415954-9. DOI: https://doi.org/10.1016/B978-0-12-415954-9.00001-2. URL: https://www.sciencedirect.com/science/article/pii/B9780124159549000012.

[12] Kun Du et al. "Effects of the Ribbed-Squealer Tip on the Blade Tip Aerothermal Performance in a High Pressure Gas Turbine Cascade". In: *urbomachinery Technical Conference and Exposition* (Oct. 2022). DOI: 10.1115/GT2022-81569.

[13] John A Ekaterinaris. "Prediction of active flow control performance on airfoils and wings". In: *Aerospace Science and Technology* 8.5 (2004), pp. 401–410. ISSN: 1270-9638. DOI: https://doi.org/10.1016/j.ast.2004.02.003. URL: https://www.sciencedirect.com/science/article/pii/S1270963804000148.

[14] W.E. Forsthoffer. "6 - Gas Turbine Best Practices". In: *Forsthoffer's Best Practice Handbook for Rotating Machinery*. Ed. by W.E. Forsthoffer. Boston: Butterworth-Heinemann, 2011, pp. 313–346. ISBN: 978-0-08-096676-2. DOI: https://doi.org/10.1016/B978-0-08-096676-2.10006-2. URL: https://www.sciencedirect.com/science/article/pii/B9780080966762100062.

[15] *Gas Turbine Power Plant with Regeneration, Reheating and Intercooling*. Accessed September 2018. 2018. URL: https://basicmechanicalengineering.com/gas-turbine-power-plant-with-regeneration-reheatintercooling/.

[16] Martin Neil Goodhand. *COMPRESSOR LEADING EDGES*. 2010.

[17] Paul C. Hanlon. “Compressor Performance – Positive Displacement”. In: 1st ed. Vol. 1. McGraw-Hill Companies, 2001, pp. 53–55.

[18] Howard H. Ho et al. “Synthetic Jet Actuators for Active Flow Control: A Review”. In: *Fluids* 9.12 (2024). ISSN: 2311-5521. DOI: 10.3390/fluids9120290. URL: https://www.mdpi.com/2311-5521/9/12/290.

[19] Davoud Hosseinzadeh, Esmail Lakzian, and Sławomir Dykas. “Optimization of the Trailing Edge Inclination of Wet Steam Turbine Stator Blade Towards the Losses Reduction”. In: *Experimental Techniques* 47 (Jan. 2022). DOI: 10.1007/s40799-021-00534-5.

[20] Robert Jaron et al. *Optimization of Trailing-Edge Serrations to Reduce Open-Rotor Tonal Interaction Noise Optimization of Trailing-Edge Serrations to Reduce Open-Rotor Tonal Interaction Noise O N R O TATIN G M ISROMAC 2016 International Symposium on Transport Phenomena and Dynamics of Rotating Machinery*. URL: https://hal.science/hal-01884252v1.

[21] Earl Logan. *Handbook of Turbomachinery*. Marcel Dekker, 1995.

[22] Kevin J Melcher and Javier A Kypuros. *Toward a Fast-Response Active Turbine Tip Clearance Control*. 2004. URL: http://www.sti.nasa.gov.

[23] Peyman Ghashghaie Nejad and Reza Taghavi Zenouz. “Axial compressor blades tip leakage flow control using natural aspiration”. In: *Scientific Reports* 13 (1 Dec. 2023). ISSN: 20452322. DOI: 10.1038/s41598-023-49391-9.

[24] Andrew Parr. “Chapter — three - Air Compressors, Air Treatment and Pressure Regulation”. In: *Hydraulics and Pneumatics (Third Edition)*. Third Edition. Oxford: Butterworth-Heinemann, 2011, pp. 51–73. ISBN: 978-0-08-096674-8. DOI: https://doi.org/10.1016/B978-0-08-096674-8.00003-3. URL: https://www.sciencedirect.com/science/article/pii/B9780080966748000033.

[25] R. Rayner. “FLUID MECHANICS PRINCIPLES”. In: *Pump Users Handbook (Fourth Edition)*. Ed. by R. Rayner. Fourth Edition. Amsterdam: Elsevier Science, 1995, pp. 1–22. ISBN: 978-1-85617-216-5. DOI: https://doi.org/10.1016/B978-185617216-5/50002-3. URL: https://www.sciencedirect.com/science/article/pii/B9781856172165500023.

[26] Nilesh P Salunke and S A Channiwala. *Original Paper Design and Analysis of a Controlled Diffusion Aerofoil Section for an Axial Compressor Stator and Effect of Incidence Angle and Mach No. on Performance of CDA*.

[27] Pasquale M. Sforza. “Chapter 8 - Blade Element Theory for Axial Flow Turbomachines”. In: *Theory of Aerospace Propulsion*. Ed. by Pasquale M. Sforza. Aerospace Engineering. Boston: Butterworth-Heinemann, 2012, pp. 307–357. ISBN: 978-1-85617-912-6. DOI: https://doi.org/10.1016/B978-1-85617-912-

6.00008-6. URL: https://www.sciencedirect.com/science/article/pii/B9781856179126000086.

[28] Richard E. Sonntag and Claus Borgnakke. *Introduction to Engineering Thermodynamics*. 2nd. John Wiley, 2006. ISBN: 9780471737599.

[29] Bruce M Steinetz et al. *Evaluation of an Active Clearance Control System Concept*. 2005. URL: http://www.sti.nasa.gov.

[30] Vandad Talimi. *Mechanical Equipment and Systems*. Original author unknown. 2013. URL: http://www.engr.mun.ca/~yuri/Courses/MechanicalSystems/Turbomachinery.pdf.

[31] Ting Wang. "15 - The gas and steam turbines and combined cycle in IGCC systems". In: *Integrated Gasification Combined Cycle (IGCC) Technologies*. Ed. by Ting Wang and Gary Stiegel. Woodhead Publishing, 2017, pp. 497–640. ISBN: 978-0-08-100167-7. DOI: https://doi.org/10.1016/B978-0-08-100167-7.00028-7. URL: https://www.sciencedirect.com/science/article/pii/B9780081001677000287.

[32] David W. Wragg. *A Dictionary of Aviation*. 1st. Osprey, 1973, p. 141. ISBN: 9780850451634.

Appendix A

MATLAB Code Listings for Velocity Triangles and Schematics of Engine Stages

Corresponding to the velocity triangles of absolute and relative velocity at the compressor inlet and outlet, the solution has been evaluated in 4.1 and 4.2 whereas following listings displays the MATLAB codes devising for obtaining the velocity triangles, blade profiles, integrated systems.

```
    % Velocity Triangle Plot for Axial Compressor
clear;
clf;
hold on;
axis equal;
% Preliminary Data
V1 = 163;
alpha1 = 13; % Inlet angle
Vx = V1 * cosd(alpha1);
Vu1 = V1 * sind(alpha1);
U = 301;
Vu2 = 264.34;
Vx2 = Vx; % constant axial velocity
Vu_rel1 = U - Vu1;
Vu_rel2 = U - Vu2;
W1 = sqrt(Vx^2 + Vu_rel1^2);
beta1 = atand(Vx / Vu_rel1);
W2 = sqrt(Vx^2 + Vu_rel2^2);
beta2 = atand(Vx / Vu_rel2);
% Origin
O = [0 0];
```

```
% Vector endpoints
V1_vec = [Vx Vu1];
W1_vec = [Vx -Vu_rel1];
U_vec = [0 U];
V2_vec = [Vx Vu2];
W2_vec = [Vx -Vu_rel2];
% Plot inlet triangle
quiver(O(1),O(2), V1_vec(1), V1_vec(2), 0, 'r','LineWidth',2,'
    MaxHeadSize',0.5);
quiver(O(1),O(2), Vx, 0, 0, 'g','LineWidth',2,'MaxHeadSize',0.5);
quiver(O(1),O(2), 0, Vu1, 0, 'b','LineWidth',2,'MaxHeadSize',0.5);
quiver(O(1)+Vx,0, 0, Vu1, 0,'b','LineStyle','--');
% Relative velocity inlet
quiver(O(1),O(2), Vx, -Vu_rel1, 0, 'm','LineWidth',2,'MaxHeadSize',0.5);
% Blade speed U
quiver(O(1),O(2), 0, U, 0, 'k','LineWidth',2,'MaxHeadSize',0.5);
% Plot outlet triangle shifted
offset = [400 0]; % shift right for clarity
quiver(offset(1),offset(2), V2_vec(1), V2_vec(2), 0, 'r','LineWidth',2,'
    MaxHeadSize',0.5);
quiver(offset(1),offset(2), Vx2, 0, 0, 'g','LineWidth',2,'MaxHeadSize'
    ,0.5);
quiver(offset(1),offset(2), 0, Vu2, 0, 'b','LineWidth',2,'MaxHeadSize'
    ,0.5);
quiver(offset(1)+Vx2,0, 0, Vu2, 0,'b','LineStyle','--');
% Relative velocity outlet
quiver(offset(1),offset(2), Vx2, -Vu_rel2, 0, 'm','LineWidth',2,'
    MaxHeadSize',0.5);
% Blade speed U at outlet
quiver(offset(1),offset(2), 0, U, 0, 'k','LineWidth',2,'MaxHeadSize'
    ,0.5);
% Labels
text(V1_vec(1)/2, V1_vec(2)/2 + 10, 'V_1','Color','r','FontSize',12);
text(Vx/2 - 10, -15, 'V_x','Color','g','FontSize',12);
text(-30, Vu1/2, 'V_{u1}','Color','b','FontSize',12);
text(Vx, -Vu_rel1/2, 'W_1','Color','m','FontSize',12);
text(-30, U/2, 'U','Color','k','FontSize',12);
text(offset(1) + V2_vec(1)/2, offset(2) + V2_vec(2)/2 + 10, 'V_2','Color
    ','r','FontSize',12);
text(offset(1) + Vx2/2 - 10, offset(2) - 15, 'V_x','Color','g','FontSize
    ',12);
text(offset(1) - 30, offset(2) + Vu2/2, 'V_{u2}','Color','b','FontSize'
    ,12);
text(offset(1) + Vx2, offset(2) - Vu_rel2/2, 'W_2','Color','m','FontSize
    ',12);
text(offset(1) - 30, offset(2) + U/2, 'U','Color','k','FontSize',12);
title('Velocity Triangles at Compressor Inlet and Outlet');
```

```
xlabel('Axial Direction');
ylabel('Tangential Direction');
grid on;
```

Listing A.1: MATLAB code for evaluation of inlet and outlet velocity triangles of compressor

```
    % Schematic of compressor blade cross-section
clear;
clf;
hold on;
axis equal;
title('Compressor Blade Cross-Section');
% Chord line
chord = 1; % arbitrary unit
plot([0 chord], [0 0], 'k', 'LineWidth', 1.5);
% Camber line
theta = linspace(0, pi, 100);
camber_radius = 2; % radius of camber arc
x_camber = chord * (1 - cos(theta))/2;
y_camber = camber_radius - sqrt(camber_radius^2 - (x_camber - chord/2)
    .^2);
plot(x_camber, y_camber, 'b', 'LineWidth', 1.5);
% Leading and trailing edge thickness
plot([0 0], [-0.02 0.02], 'r', 'LineWidth', 1.5); % leading edge
plot([chord chord], [-0.015 0.015], 'r', 'LineWidth', 1.5); % trailing
    edge
% Labels
text(0, -0.05, 'Leading Edge','HorizontalAlignment','center');
text(chord, -0.05, 'Trailing Edge','HorizontalAlignment','center');
text(chord/2, 0.1, 'Camber Line','Color','b');
xlabel('Chordwise Direction');
ylabel('Blade Thickness');
xlim([-0.1 chord+0.1]);
ylim([-0.1 0.2]);
grid on;
```

Listing A.2: MATLAB code for devising cross-sectional view of compressor blade

```
    % Compressor Blade Cross-Section Schematic
clear; clf; hold on; axis equal;
title('Axial Compressor Blade Cross-Section');

% Chord length
chord = 1; % normalized

% Generate camber line (lower camber for compressor)
theta = linspace(0, pi, 100);
```

```
camber_radius = 2.5; % larger radius = lower camber
x_camber = chord * (1 - cos(theta))/2;
y_camber = camber_radius - sqrt(camber_radius^2 - (x_camber - chord/2)
    .^2);
% Defining blade thickness (less than turbine blade)
thickness = 0.04 * (1 - cos(pi * x_camber / chord));
% Create pressure and suction sides
x_upper = x_camber;
y_upper = y_camber + thickness/2;
y_lower = y_camber - thickness/2;
x_lower = x_upper; % same chordwise coordinates
% Plotting blade shape (filled)
fill([x_upper fliplr(x_lower)], [y_upper fliplr(y_lower)], [0.8 0.9 1]);
     % light blue fill
% Plotting camber line
plot(x_camber, y_camber, 'b--', 'LineWidth', 1.2);
% Plotting chord line
plot([0 chord], [0 0], 'k', 'LineWidth', 1.2);
% Leading and trailing edge markers
plot([0 0], [-0.015 0.015], 'r', 'LineWidth', 1.2);
plot([chord chord], [-0.01 0.01], 'r', 'LineWidth', 1.2);
% Labelling
text(0, -0.04, 'Leading Edge','HorizontalAlignment','center');
text(chord, -0.04, 'Trailing Edge','HorizontalAlignment','center');
text(chord/2, 0.1, 'Camber Line','Color','b');
text(x_upper(end/3), y_upper(end/3)+0.015, 'Suction Side');
text(x_lower(end/3), y_lower(end/3)-0.015, 'Pressure Side');
xlabel('Chordwise Direction');
ylabel('Blade Height');
xlim([-0.1 chord+0.1]);
ylim([-0.1 0.15]);
grid on;
```

Listing A.3: MATLAB code for devsiing of compressor blade cross-sectional view

```
    % Turbine Velocity Triangle Plot (Inlet and Outlet)
clear;
clf; hold on;
axis equal;
title('Turbine Velocity Triangles (Inlet and Outlet)');
% Given values
U_t = 301; % Blade speed (m/s)
V1t = 345; % Absolute inlet velocity (m/s)
alpha1t = 29; % Inlet absolute angle (degrees)
Vx_t = V1t * cosd(alpha1t); % Axial component
Vu1t = V1t * sind(alpha1t); % Tangential component
Vu2t = -130.9027; % Exit tangential velocity (negative)
% Same axial velocity assumed
```

```
% Relative velocities
W1t = sqrt(Vx_t^2 + (U_t - Vu1t)^2);
W2t = sqrt(Vx_t^2 + (U_t - Vu2t)^2);
% Relative inlet angle
beta1t = atan2d(Vx_t, (U_t - Vu1t));
% Relative outlet angle
beta2t = atan2d(Vx_t, (U_t - Vu2t));
%  Inlet Triangle (origin)
O = [0 0];
% Absolute inlet vector
V1t_vec = [Vx_t Vu1t];
% Relative inlet vector
W1t_vec = [Vx_t -(U_t - Vu1t)];
% Blade speed vector
U_vec = [0 U_t];
% Plotting of inlet absolute velocity
quiver(O(1),O(2), V1t_vec(1), V1t_vec(2), 0, 'r','LineWidth',2,'
    MaxHeadSize',0.5);
% Plot axial component
quiver(O(1),O(2), Vx_t, 0, 0, 'g','LineWidth',2,'MaxHeadSize',0.5);
% Plotting of tangential inlet
quiver(O(1),O(2), 0, Vu1t, 0, 'b','LineWidth',2,'MaxHeadSize',0.5);
% Plot relative inlet velocity
quiver(O(1),O(2), Vx_t, -(U_t - Vu1t), 0, 'm','LineWidth',2,'MaxHeadSize
    ',0.5);
% Plotting of blade speed
quiver(O(1),O(2), 0, U_t, 0, 'k','LineWidth',2,'MaxHeadSize',0.5);
%  Outlet Triangle
offset = [450 0];
% Absolute outlet vector
V2t_vec = [Vx_t Vu2t];
% Relative outlet vector
W2t_vec = [Vx_t -(U_t - Vu2t)];
% Plotting of outlet absolute velocity
quiver(offset(1),offset(2), V2t_vec(1), V2t_vec(2), 0, 'r','LineWidth'
    ,2,'MaxHeadSize',0.5);
% Plot axial component
quiver(offset(1),offset(2), Vx_t, 0, 0, 'g','LineWidth',2,'MaxHeadSize'
    ,0.5);
% Plotting of tangential outlet
quiver(offset(1),offset(2), 0, Vu2t, 0, 'b','LineWidth',2,'MaxHeadSize'
    ,0.5);
% Plot relative outlet velocity
quiver(offset(1),offset(2), Vx_t, -(U_t - Vu2t), 0, 'm','LineWidth',2,'
    MaxHeadSize',0.5);
% Plotting of blade speed
```

```
quiver(offset(1),offset(2), 0, U_t, 0, 'k','LineWidth',2,'MaxHeadSize',0.5);
%Labels for Inlets
text(V1t_vec(1)/2, V1t_vec(2)/2 + 15, 'V_{1t}','Color','r','FontSize',12);
text(Vx_t/2 - 20, -20, 'V_x','Color','g','FontSize',12);
text(-35, Vu1t/2, 'V_{u1t}','Color','b','FontSize',12);
text(Vx_t, -(U_t - Vu1t)/2, 'W_{1t}','Color','m','FontSize',12);
text(-25, U_t/2, 'U','Color','k','FontSize',12);
% Labels for Outlet
text(offset(1) + V2t_vec(1)/2, offset(2) + V2t_vec(2)/2 + 15, 'V_{2t}','Color','r','FontSize',12);
text(offset(1) + Vx_t/2 - 20, offset(2) - 20, 'V_x','Color','g','FontSize',12);
text(offset(1)-35, offset(2) + Vu2t/2, 'V_{u2t}','Color','b','FontSize',12);
text(offset(1) + Vx_t, offset(2) - (U_t - Vu2t)/2, 'W_{2t}','Color','m','FontSize',12);
text(offset(1)-25, offset(2) + U_t/2, 'U','Color','k','FontSize',12);
xlabel('Axial Direction');
ylabel('Tangential Direction');
xlim([-50 offset(1)+Vx_t+100]);
ylim([-200 400]);
grid on;
```

Listing A.4: MATLAB code for evaluation of inlet and outlet velocity triangles of turbine

```
    % Turbine Velocity Triangles by Overlaying of plots at Hub, Mean, Tip
clear;
clf; hold on;
axis equal;
title('Overlay of Turbine Velocity Triangles about Hub, Mean, Tip (Free Vortex)');
% Constants
V1t = 345; % Absolute inlet velocity (m/s)
alpha1t = 29; % Inlet absolute angle (deg)
Vx_t = V1t * cosd(alpha1t);
Vu1t_m = V1t * sind(alpha1t);
% Radii
r_h = 0.2; r_m = 0.3; r_t = 0.4;
K = Vu1t_m * r_m; % free vortex constant
% Tangential velocities
Vu1t_h = K / r_h;
Vu1t_m = K / r_m; % same as original
Vu1t_t = K / r_t;
% Evaluation of Blade speeds
```

```
U_h = 301 * r_h / r_m;
U_m = 301; % design at mean radius
U_t = 301 * r_t / r_m;
% Computation of relative velocities
W1t_h = sqrt(Vx_t^2 + (U_h - Vu1t_h)^2);
W1t_m = sqrt(Vx_t^2 + (U_m - Vu1t_m)^2);
W1t_t = sqrt(Vx_t^2 + (U_t - Vu1t_t)^2);
% Angles
beta1t_h = atan2d(Vx_t, U_h - Vu1t_h);
beta1t_m = atan2d(Vx_t, U_m - Vu1t_m);
beta1t_t = atan2d(Vx_t, U_t - Vu1t_t);
% Defination of colors
colors = {'r','g','b'};
labels = {'Hub','Mean','Tip'};
offsets = [0 500 1000]; % shift triangles horizontally
for i = 1:3
    % Assign radius-based variables
    if i == 1
        Vu = Vu1t_h; U = U_h; W = W1t_h; beta = beta1t_h;
    elseif i == 2
        Vu = Vu1t_m; U = U_m; W = W1t_m; beta = beta1t_m;
    else
        Vu = Vu1t_t; U = U_t; W = W1t_t; beta = beta1t_t;
    end
    offset = offsets(i);
    % Absolute velocity components
    V_abs = [Vx_t Vu];
    % Relative velocity components
    W_rel = [Vx_t -(U - Vu)];
    % Plotting of absolute velocity
    quiver(offset,0, V_abs(1), V_abs(2), 0, colors{i},'LineWidth',2,'
    MaxHeadSize',0.5);
    % Plotting of axial component
    quiver(offset,0, Vx_t, 0, 0, 'k','LineWidth',1.5,'MaxHeadSize',0.5);
    % Plotting of tangential component
    h = quiver(offset,0, 0, Vu, 0, 'LineWidth',1.5,'MaxHeadSize',0.5);
h.Color = [0.5 0.5 0.5];
    % Plotting of relative velocity
    quiver(offset,0, W_rel(1), W_rel(2), 0, colors{i},'LineStyle','--','
    LineWidth',2,'MaxHeadSize',0.5);
    % Plotting of blade speed
    quiver(offset,0, 0, U, 0, 'm','LineWidth',1.5,'MaxHeadSize',0.5);
    % Labelling
    text(offset + V_abs(1)/2, V_abs(2)/2 + 20, sprintf('V_{1t} %s',
    labels{i}),'Color',colors{i});
    text(offset + Vx_t/2 - 20, -20, 'V_x','Color','k');
```

```
    text(offset - 40, Vu/2, sprintf('V_{u1t} %s',labels{i}),'Color',[0.5
     0.5 0.5]);
    text(offset + W_rel(1), W_rel(2)-20, sprintf('W_{1t} %s',labels{i}),
    'Color',colors{i});
    text(offset - 30, U/2, 'U','Color','m');
end
xlabel('Axial Direction');
ylabel('Tangential Direction');
xlim([-50 offsets(3)+Vx_t+200]);
ylim([-250 450]);
grid on;
legend('Hub','Mean','Tip','Location','northwest');
```

Listing A.5: MATLAB code for overlaying of velocity triangles about hub,rotor and mean radius

```
    % Turbine Blade Cross-Section Schematic
clear; clf; hold on; axis equal;
title('Axial Turbine Blade Cross-Section');
% Chord length
chord = 1; % normalized
% Generation of camber line (higher camber than compressor)
theta = linspace(0, pi, 100);
camber_radius = 1.5; % smaller radius = higher camber
x_camber = chord * (1 - cos(theta))/2;
y_camber = camber_radius - sqrt(camber_radius^2 - (x_camber - chord/2)
    .^2);
% Defining of blade thickness (typically more at leading edge in
    turbines)
thickness = 0.07 * (1 - cos(pi * x_camber / chord));
% Creation of pressure and suction sides
x_upper = x_camber;
y_upper = y_camber + thickness/2;
y_lower = y_camber - thickness/2;
x_lower = x_upper;
% Plotting blade shape (filled)
fill([x_upper fliplr(x_lower)], [y_upper fliplr(y_lower)], [1 0.9 0.7]);
     % light orange fill
% Plotting camber line
plot(x_camber, y_camber, 'b--', 'LineWidth', 1.2);
% Plotting chord line
plot([0 chord], [0 0], 'k', 'LineWidth', 1.2);
% Leading and trailing edge thickness markers
plot([0 0], [-0.02 0.02], 'r', 'LineWidth', 1.5);
plot([chord chord], [-0.015 0.015], 'r', 'LineWidth', 1.5);
% Labelling
text(0, -0.05, 'Leading Edge','HorizontalAlignment','center');
text(chord, -0.05, 'Trailing Edge','HorizontalAlignment','center');
```

```
text(chord/2, 0.12, 'Camber Line','Color','b');
text(x_upper(end/3), y_upper(end/3)+0.02, 'Suction Side');
text(x_lower(end/3), y_lower(end/3)-0.02, 'Pressure Side');
xlabel('Chordwise Direction');
ylabel('Blade Height');
xlim([-0.1 chord+0.1]);
ylim([-0.1 0.2]);
grid on;
```

Listing A.6: MATLAB code for devsiing turbine blade cross-section

```

clear;
clf;
hold on;
axis equal;
title('Schematic of Engine Stages: Compressor and Turbine Blades');
% Chord length for blades
chord = 1;
%For compressor: The camber radius and specification of thickness
camber_radius_c = 2.5; % low camber
theta = linspace(0, pi, 100);
x_camber_c = chord * (1 - cos(theta))/2;
y_camber_c = camber_radius_c - sqrt(camber_radius_c^2 - (x_camber_c -
    chord/2).^2);
thickness_c = 0.06 * (1 - cos(pi * x_camber_c / chord)); % increased
    thickness
x_upper_c = x_camber_c; y_upper_c = y_camber_c + thickness_c/2;
y_lower_c = y_camber_c - thickness_c/2; x_lower_c = x_upper_c;
%For turbine: The camber radius and specification of thickness
camber_radius_t = 1.5; % higher camber
x_camber_t = chord * (1 - cos(theta))/2;
y_camber_t = camber_radius_t - sqrt(camber_radius_t^2 - (x_camber_t -
    chord/2).^2);
thickness_t = 0.1 * (1 - cos(pi * x_camber_t / chord)); % increased
    thickness
x_upper_t = x_camber_t; y_upper_t = y_camber_t + thickness_t/2;
y_lower_t = y_camber_t - thickness_t/2; x_lower_t = x_upper_t;
% Scaling of blade heights
scale_factor = 2.5; % adjust for visibility
y_upper_c = y_upper_c * scale_factor;
y_lower_c = y_lower_c * scale_factor;
y_camber_c = y_camber_c * scale_factor;
y_upper_t = y_upper_t * scale_factor;
y_lower_t = y_lower_t * scale_factor;
y_camber_t = y_camber_t * scale_factor;
% Stage counts
N_compressor = 3;
```

```
N_turbine = 4;
spacing = 2;
%Plotting of coompressor blades
for i = 0:N_compressor-1
    offset_x = i * spacing;
    fill(offset_x + [x_upper_c fliplr(x_lower_c)], [y_upper_c fliplr(
    y_lower_c)], [0.8 0.9 1]);
    plot(offset_x + x_camber_c, y_camber_c, 'b--', 'LineWidth', 1);
end
%Combusion chamber
combustor_start = N_compressor * spacing + 0.4;
combustor_length = 1;
combustor_height = 1.0;
rectangle('Position', [combustor_start, -combustor_height/2,
    combustor_length, combustor_height], ...
    'FaceColor', [0.9 0.9 0.9], 'EdgeColor', 'k');
text(combustor_start + combustor_length/2, -1.3, 'Combustor', '
    HorizontalAlignment', 'center');
%Plotting of mirrored turbine blades
for i = 0:N_turbine-1
    offset_x = combustor_start + combustor_length + (i+1) * spacing;
    fill(offset_x - [x_upper_t fliplr(x_lower_t)], -[y_upper_t fliplr(
    y_lower_t)], [1 0.9 0.7]);
    plot(offset_x - x_camber_t, -y_camber_t, 'b--', 'LineWidth', 1);
end
% Flow arrows
arrow_y = 0;
arrow_length = spacing * 0.8;
for i = 0:(N_compressor + N_turbine + 2)
    quiver(i * spacing, arrow_y, arrow_length, 0, 0, 'k', 'MaxHeadSize',
     0.5, 'LineWidth', 1.5);
end
%Stage labelling
text(spacing * (N_compressor/2), scale_factor*0.9, 'Compressor Stage', '
    FontWeight', 'bold', 'HorizontalAlignment', 'center');
text(combustor_start + combustor_length/2, scale_factor*0.9, 'Combustion
     Chamber', 'FontWeight', 'bold', 'HorizontalAlignment', 'center');
text(combustor_start + combustor_length + spacing * (N_turbine/2), -
    scale_factor*1.2, 'Turbine Stage', 'FontWeight', 'bold', '
    HorizontalAlignment', 'center');
xlabel('Axial Direction');
ylabel('Relative Blade Height');
xlim([-0.2 combustor_start + combustor_length + N_turbine * spacing +
    1]);
ylim([-scale_factor*1.5 scale_factor*1.5]);
grid on;
```

Listing A.7: MATLAB code for engine stage comprsing of compressor and turbine

```
    % Integrated Engine System Schematic
clear;
clf;
hold on;
axis equal;
title('Integrated Engine System Schematic');
% Chord length
chord = 1;
% Compressor blade geometry
camber_radius_c = 2.5;
theta = linspace(0, pi, 100);
x_camber_c = chord * (1 - cos(theta))/2;
y_camber_c = camber_radius_c - sqrt(camber_radius_c^2 - (x_camber_c -
    chord/2).^2);
thickness_c = 0.06 * (1 - cos(pi * x_camber_c / chord));
x_upper_c = x_camber_c;
y_upper_c = y_camber_c + thickness_c/2;
y_lower_c = y_camber_c - thickness_c/2;
x_lower_c = x_upper_c;
% Turbine blade geometry
camber_radius_t = 1.5;
x_camber_t = chord * (1 - cos(theta))/2;
y_camber_t = camber_radius_t - sqrt(camber_radius_t^2 - (x_camber_t -
    chord/2).^2);
thickness_t = 0.1 * (1 - cos(pi * x_camber_t / chord));
x_upper_t = x_camber_t;
y_upper_t = y_camber_t + thickness_t/2;
y_lower_t = y_camber_t - thickness_t/2;
x_lower_t = x_upper_t;
% Scaling of blades for visibility
scale_factor = 2.5;
y_upper_c = y_upper_c * scale_factor;
y_lower_c = y_lower_c * scale_factor;
y_camber_c = y_camber_c * scale_factor;
y_upper_t = y_upper_t * scale_factor;
y_lower_t = y_lower_t * scale_factor;
y_camber_t = y_camber_t * scale_factor;
% Stage counts
N_compressor = 4;
N_turbine = 3;
spacing = 2.5;
% Plotting of compressor blades
for i = 0:N_compressor-1
    offset_x = i * spacing;
    fill(offset_x + [x_upper_c fliplr(x_lower_c)], [y_upper_c fliplr(
    y_lower_c)], [0.8 0.9 1]);
    plot(offset_x + x_camber_c, y_camber_c, 'b--', 'LineWidth', 1);
```

```
end
% Integration of Combustor
combustor_start = N_compressor * spacing + 0.4;
combustor_length = 1;
combustor_height = 1.0;
rectangle('Position', [combustor_start, -combustor_height/2,
    combustor_length, combustor_height], ...
    'FaceColor', [0.9 0.9 0.9], 'EdgeColor', 'k');
text(combustor_start + combustor_length/2, -1.3, 'Combustor', '
    HorizontalAlignment', 'center');
% Plotting of turbine blades (mirrored)
for i = 0:N_turbine-1
    offset_x = combustor_start + combustor_length + (i+1) * spacing;
    fill(offset_x - [x_upper_t fliplr(x_lower_t)], -[y_upper_t fliplr(
    y_lower_t)], [1 0.9 0.7]);
    plot(offset_x - x_camber_t, -y_camber_t, 'b--', 'LineWidth', 1);
end
% Flow arrows across system
arrow_y = scale_factor*1.1;
arrow_length = spacing * 0.8;
for i = 0:(N_compressor + N_turbine + 2)
    quiver(i * spacing, arrow_y, arrow_length, 0, 0, 'k', 'MaxHeadSize',
     0.5, 'LineWidth', 1.5);
end
% Mechanical coupling arrow (shaft connecting turbine to compressor)
x_shaft_start = combustor_start + combustor_length + spacing * N_turbine
    ;
x_shaft_end = spacing * N_compressor;
y_shaft = -scale_factor*1.5;
plot([x_shaft_start x_shaft_end], [y_shaft y_shaft], 'k-', 'LineWidth',
    2);
quiver(x_shaft_start, y_shaft, -(x_shaft_start - x_shaft_end)*0.9, 0, 0,
     'k', 'MaxHeadSize', 0.8, 'LineWidth', 2);
text((x_shaft_start+x_shaft_end)/2, y_shaft-0.5, 'Mechanical Shaft (
    Turbine Drives Compressor)', 'HorizontalAlignment', 'center');
% Labels: stages
text(spacing * (N_compressor/2), scale_factor*2.0, 'Compressor Stage', '
    FontWeight', 'bold', 'HorizontalAlignment', 'center');
text(combustor_start + combustor_length/2, scale_factor*2.0, 'Combustion
     Chamber', 'FontWeight', 'bold', 'HorizontalAlignment', 'center');
text(combustor_start + combustor_length + spacing * (N_turbine/2), -
    scale_factor*2.3, 'Turbine Stage', 'FontWeight', 'bold', '
    HorizontalAlignment', 'center');
% Thermodynamic state labelling
text(spacing*0.2, scale_factor*1.5, 'T_{01}, P_{01}', 'FontSize', 10);
text(spacing*N_compressor-0.5, scale_factor*1.5, 'T_{02}, P_{02}', '
    FontSize', 10);
```

```
text(combustor_start+0.1, scale_factor*1.5, 'T_{03}, P_{03}', 'FontSize', 10);
text(combustor_start + combustor_length + spacing*0.5, scale_factor*1.5, 'T_{04}, P_{04}', 'FontSize', 10);
% Work balance symbols
text(spacing*N_compressor*0.5, -scale_factor*2.2, 'W_c', 'FontSize', 12, 'FontWeight', 'bold');
text(combustor_start + combustor_length + spacing*(N_turbine/2), -scale_factor*2.2, 'W_t', 'FontSize', 12, 'FontWeight', 'bold');
xlabel('Axial Direction');
ylabel('Relative Blade Height');
xlim([-0.5 combustor_start + combustor_length + N_turbine * spacing + 1]);
ylim([-scale_factor*3 scale_factor*3]);
grid on;
```

Listing A.8: MATLAB code for integrated engine system schematic with necessary annotations

Appendix B

Project Management

The Preliminary Design and Analysis of an Axial Compressor and Matching Turbine Stage for a Gas Turbine research-oriented project not only highlights the technical accomplishments but also effective project management under constrained timelines and academic deliverables. Some important aspects are highlighted as follows:

1. Milestone Tracking: The project complied with the predefined parameters associated with the compressor design, turbine design, integrated analysis, and documentation phases,thereby enabling for effective and progressive validation of each stage.

2. Task Prioritization and Iterative Refinement: In order to balance the theoretical derivations, MATLAB code development for plotting of figures, a matrix was predefined which aimed at iterative refinement of document ensuing accuracy and high presentation quality.

3. Identification and Mitigation of Associated Risks: During the entire analysis, some potential risks—such as misalignment between turbine and compressor work, coding errors, and schematic inaccuracies were identified progressively and rectified at earliest. Verification measures such as independent hand calculations, and MATLAB visualization checks were implemented.

4. Resource Management: The project maximized the available academic resources (supervisor consultation, literature databases, MATLAB toolboxes, LaTeXrefinement) while managing computational limitations and available time.

Appendix C

Project Log

The following is a weekly summary of the work carried during the development of this body of work. It covers tasks that were completed, tutorials that were worked through, articles that were read and reviews of discussions / meetings held with the project supervisor and other third parties.

Day 1: Thursday 01/05/2025

First day working on the project. Underwent significant literature review and selected the most optimum LaTeXtemplate for devising the report.

- Proceeded with the project deliverable and deliberated to highlight the major aspects of analysis
- Initiated the project by devising objectives and scope of project initially to provide a road map to follow through the entire course.
- Consulted over 15 literature items, from conferences to journals and books to work on the introduction
- Manually evaluated the solutions corresponding to 4.1 and 4.2 before implementing the calculations in LaTeX
- Completed 4.1 and 4.2 in the course of approximately 13 hours.
- Worked on MATLAB scripts for devising the velocity triangles for the compressor and turbine and worked on overlaying of triangles when the analysis about hub, tip and mean radius was concerned

Day 2: Friday 02/05/2025

Had a meeting with supervisor and discussed some of the issues related to the project. After obtaining his consent, further work was initiated

- Worked on MATLAB codes for devising cross-sectional views of compressor and turbine blades by deliberating into the necessary aspects.
- Constructed the engine configuration in MATLAB by rigorous hit and trials until adequate form was achieved.
- Most theoretical work was completed, especially 4.4 and 4.3
- 5 was devised thus ending approximately 20 hour toil on the project